

A  
DISSERTATION REPORT  
ON  
**STUDIES ON STATIONARY CI ENGINE EXHAUST HEAT RECOVERY  
UNIT**

Submitted in partial fulfillment of the requirements for the award of the degree of

**MASTER IN TECHNOLOGY  
IN  
THERMAL ENGINEERING**



Submitted by  
**SWARAJ DAS**  
2015PTE5078

Supervisor  
**Prof. Dilip Sharma**

**DEPARTMENT OF MECHANICAL ENGINEERING  
MALAVIYA NATIONAL INSTITUTE OF TECHNOLOGY JAIPUR  
JUNE 2017**

**© MALAVIYA NATIONAL INSTITUTE OF TECHNOLOGY JAIPUR  
ALL RIGHTS RESERVED**



**MALAVIYA NATIONAL INSTITUTE OF  
TECHNOLOGY JAIPUR  
DEPARTMENT OF MECHANICAL ENGINEERING  
JAIPUR- 302017, RAJASTHAN, INDIA**

**CERTIFICATE**

This is to certify that the dissertation report entitled **“STUDIES ON STATIONARY C.I. ENGINE EXHAUST HEAT RECOVERY UNIT”** being submitted by **SWARAJ DAS (2015PTE5078)**, in partial fulfillment of the requirement for the award of the degree of **Master of Technology in Thermal Engineering** of Malaviya National Institute of Technology Jaipur is a record of bonafide research work carried out by him under my supervision. The contents of this dissertation work in full or in parts have not been submitted to any other institute or university for the award of any degree or diploma.

Date:

Place:

**Prof. Dilip Sharma**

Department of Mechanical Engineering  
Malaviya National Institute of Technology  
Jaipur -302017, Rajasthan



**MALAVIYA NATIONAL INSTITUTE OF  
TECHNOLOGY JAIPUR  
DEPARTMENT OF MECHANICAL ENGINEERING  
JAIPUR- 302017, RAJASTHAN, INDIA**

---

**DECLARATION**

---

I **Swaraj Das**, declare that the dissertation report entitled “**STUDIES ON STATIONARY C.I. ENGINE EXHAUST HEAT RECOVERY UNIT**” being submitted by me in partial fulfillment of the degree of **M.Tech (Thermal Engineering)** is a research work carried out by me under the supervision of **Prof. Dilip Sharma** and the contents of this dissertation report, in full or in parts, have not been submitted to any other Institute or University for the award of any degree or diploma. I also certify that no part of this seminar report has been copied or borrowed from anyone else. In case any type of plagiarism is found out, I will be solely and completely responsible for it.

Date:

Place:

**Swaraj Das**

M.Tech (Thermal Engineering)

2015PTE5078

## ACKNOWLEDGEMENT

---

---

I would like to express my sincere gratitude to **Prof. Dilip Sharma**, Professor, Department of Mechanical Engineering, who provided me with his generous guidance, valuable help and endless encouragement by taking personal interest and attention. He has been the principal motivation behind this work and provided all kind of possible support. I am very much thankful to him for his generosity and extending maximum possible help whenever required.

I want to express my deepest gratitude to **Dr. G.D. Agarwal, Dr. Nirupam Rohatagi, Dr. Jyotirmay Mathur, Prof. S. L. Soni** for showing me the right direction during the preparation of this report. Without their guidance and encouragement this work would have been impossible.

I would like to express my sincere and profound appreciation to **Mr. Dheeraj Kishor Johar**, Ph.D Research Scholar, Mechanical Engg. Dept, MNIT Jaipur, who was abundantly helpful and offered invaluable assistance, support and guidance with his experience and knowledge. I feel greatly indebted of his support, without which it would have very difficult to move ahead with my work.

I am also thankful to technical staff **Mr. Ramesh Chand Meena, Mr. Pushendra Sharma** and **Mr. Mahaveer**, Mechanical Engineering lab to provide all kind of help during my dissertation work.

I would like to thank my friends **Chandrapal Singh Inda, Nabajit Deka, Karan Yadav and C.P Chandrasekhar** for their sincere help and moral support during the entire work.

I am also immensely grateful to **Mr. Hemant Raj Singh, Mr. Sumit Sharma, Mr. Animesh K. Srivastava** and **Mr. Amit Jhalani** for their guidance and moral support during the entire work.

I wish to express my deepest gratitude to my parents for their blessings, affection and all their prayers, without which I would not be able to endure hard time and carry on.

(Swaraj Das)

## ABSTRACT

---

---

Energy plays an important role in development of any modern society or country. Increased energy demand, limited resources and the environmental pollution due to exploitation of energy, have emphasized the need for utilizing these resources more efficiently. Today's industrial developments are based upon abundant and reliable supplies of energy. The rapid industrial and economical growth in India and China, where more than one-third of the population of the world is present, has increased the need for energy in the recent years. Considering environmental protection, and in the context of the great uncertainty over future energy supplies, attention is focused on the utilization of sustainable energy sources and energy conservation methodologies.

A large quantity of hot flue gases is generated from boilers, furnaces, I.C. engines, etc. If some of this waste heat could be recovered and put into use, a considerable amount of primary fuel could be saved. Waste heat recovery (WHR) devices and cogeneration are successful energy recovery techniques to improve the overall thermal efficiency of a system to a certain extent. However, there is still a large potential to store and utilize the exit stream thermal energy by the efficient implementation of suitable WHR systems, and improvement of the overall thermal efficiency. Large capacity diesel engines are one of the most widely used power generation units. Nearly two-thirds of the input energy is wasted through the exhaust gas and cooling water of these engines. It is imperative that a serious and concrete effort should be launched for conserving this energy through waste heat recovery techniques. Such a system would ultimately reduce the overall energy requirement. Apart from the fast depleting nature of fossil fuels, the combustion of these fuels leads to considerable thermal and environmental pollution, which is threatening our eco system. The energy in the cooling water is usually considered as waste due to its low temperature level. However, much attention is focused upon the exhaust gas waste heat, and several methods are suggested to recover it. In a four stroke diesel engine, the temperature of the exhaust gas is approximately 400–550 °C at full load conditions. Hence, it is possible to recover a large quantity of useful heat from these exhaust gases.

There are various technologies to recover waste heat from the exhaust gas of internal combustion engines. These include thermoelectric generators, organic Rankine cycle, six-stroke cycle IC engine, refrigeration and air conditioning etc. The present work deals with the modeling

and simulation of a Heat Recovery Unit (HRU) for a stationary C.I. engine with the assistance of Fluent in the Ansys Workbench 15. The Heat Recovery Unit under consideration is a finned shell and tube type heat exchanger which is used to extract heat from the exhaust gas of a stationary C.I engine. In this shell and tube type heat exchanger, cylinder was made of mild steel with diameter 346 mm and height 420 mm. 45 number of tubes of diameter 18 mm were fixed in the shell. The geometry of the HRU was modeled using SOLIDWORKS which then imported into Fluent to run simulation. CFD analysis of the HRU has been carried out considering two different Energy Storage Material (ESM): Erythritol (Phase Change Material) and Shell Heat Transfer Oil S2 (Thermic Oil). The developed model was able to predict the temperature distribution inside the HRU with reasonable accuracy. The average error (between the simulation and experimental results) obtained while using thermic oil and PCM as thermal energy storage materials in the HRU are 1.01% and 2.78% respectively. Since the model is validated, the simulation results are credible.

## TABLE OF CONTENTS

|   |          |
|---|----------|
| Acknowledgement.....  | i        |
| Abstract.....   | ii       |
| Table of content.....   | iv       |
| List of Figures.....  | vii      |
| List of Tables.....   | x        |
| Nomenclature.....   | xi       |
| List of Abbreviations.....  | xii      |
| <b>1. INTRODUCTION.....</b>   | <b>1</b> |
| 1.1. Waste heat.....  | 1        |
| 1.2. Waste heat recovery.....   | 1        |
| 1.3. Waste heat recovery in internal combustion engines.....                    | 2        |
| 1.4. Advantages and disadvantages of waste heat recovery from I.C. engines..... | 3        |
| 1.4.1. Advantages of waste heat recovery.....                                   | 3        |
| 1.4.2. Disadvantages of waste heat recovery.....                                | 4        |
| 1.5. Methods of waste heat recovery.....  | 4        |
| 1.5.1. Thermoelectric generation.....   | 4        |
| 1.5.2. Organic Rankine Cycle (ORC).....   | 5        |
| 1.5.3. Turbocharging.....   | 5        |
| 1.5.4. Turbocompounding.....  | 6        |
| 1.5.5. Six- stroke internal combustion engine.....                              | 7        |
| 1.6. Outline of thesis.....   | 8        |
| <b>2. LITERATURE REVIEW.....</b>  | <b>9</b> |
| 2.1. Experimental investigations.....   | 9        |
| 2.2. Theoretical and simulation studies.....                                    | 14       |
| 2.3. Research gap based on the literature survey.....                           | 17       |
| 2.4. Objectives of the present research.....                                    | 18       |



|  |           |
|--|-----------|
| <b>3. EXPERIMENTAL SET-UP AND PROCEDURE.....</b> | <b>19</b> |
| 3.1. Diesel engine used for heat recovery.....   | 19        |
| 3.2. Dynamometer.....                            | 20        |
| 3.3. Heat recovery unit.....                     | 20        |
| 3.4. Development of experimental set-up.....     | 22        |
| 3.5. Procedure of experiment.....                | 23        |
| 3.6. Heat recovery unit insulation.....          | 24        |
| 3.7. Air flow measurement.....                   | 24        |
| 3.8. Fuel flow measurement.....                  | 26        |
| 3.9. Temperature measurement.....                | 26        |
| <b>4. CFD MODELING AND SIMULATION.....</b>       | <b>27</b> |
| 4.1. Overview of CFD simulation.....             | 27        |
| 4.1.1. Pre-processor.....                        | 27        |
| 4.1.2. Solver.....                               | 28        |
| 4.1.3. Post-processor.....                       | 28        |
| 4.2. Problem solving steps in ANSYS-FLUENT.....  | 29        |
| 4.3. CFD model development.....                  | 29        |
| 4.3.1. Geometrical modeling.....                 | 30        |
| 4.3.2. Mesh generation.....                      | 31        |
| 4.3.3. Named selection.....                      | 34        |
| 4.3.4. Assumptions taken in CFD simulation.....  | 35        |
| 4.4. CFD simulation.....                         | 35        |
| 4.4.1. Mesh quality check.....                   | 35        |
| 4.4.2. Solver.....                               | 35        |
| 4.4.3. Models.....                               | 35        |
| 4.4.4. Materials.....                            | 36        |
| 4.4.5. Boundary conditions.....                  | 36        |
| 4.4.6. Solution methods.....                     | 37        |
| 4.4.7. Solution controls.....                    | 38        |
| 4.4.8. Solution initialization.....              | 38        |

|   |           |
|---|-----------|
| <b>5. RESULTS AND DISCUSSIONS.....</b>                        | <b>39</b> |
| 5.1. Introduction.....  | 39        |
| 5.2. CASE I: THERMIC OIL AS ENERGY STORAGE MEDIUM.....        | 39        |
| 5.2.1. Experimental results during charging condition.....    | 39        |
| 5.2.2. Experimental results during discharging condition..... | 42        |
| 5.2.3. Results on simulation of HRU model.....                | 45        |
| 5.2.4. Results on validation.....                             | 49        |
| 5.3. CASE II: ERYTHRITOL AS ENERGY STORAGE MEDIUM.....        | 51        |
| 5.3.1. Experimental results during charging condition.....    | 51        |
| 5.3.2. Experimental results during discharging condition..... | 52        |
| 5.3.3. Results on simulation of HRU model.....                | 53        |
| 5.3.4. Results on validation.....                             | 57        |
| <b>6. CONCLUSION.....</b>                                     | <b>60</b> |
| 6.1. Conclusion.....  | 61        |
| 6.2. Future scope.....  | 62        |
| REFERENCES.....   | 62        |
| APPENDICES.....   | 65        |
| PUBLICATIONS.....   | 69        |

## LIST OF FIGURES

|              |  |    |
|--------------|--|----|
| Figure 1.1.  | Total fuel energy distribution in I.C. Engine.....               | 2  |
| Figure 1.2.  | Schematic of a typical TEG.....                                  | 4  |
| Figure 1.3.  | Layout of the WHR Organic Rankine Cycle.....                     | 5  |
| Figure 1.4.  | Typical turbocharger with compressor wheel and turbine.....      | 5  |
| Figure 1.5.  | Layout of Mechanical Turbocompounding.....                       | 6  |
| Figure 1.6.  | Electric Turbocompounding System.....                            | 7  |
| Figure 3.1.  | Kirloskar Diesel Engine coupled with Electrical Dynamometer..... | 19 |
| Figure 3.2.  | Photographic view of the HRU.....                                | 21 |
| Figure 3.3.  | HRU with insulation of glasswool.....                            | 21 |
| Figure 3.4.  | Converging and diverging section.....                            | 21 |
| Figure 3.5.  | Tube with fins.....  | 22 |
| Figure 3.6.  | Pictorial view of the experimental set-up.....                   | 22 |
| Figure 3.7.  | Position of tubes and thermocouples in tank.....                 | 23 |
| Figure 3.8.  | Discharging of HRU.....  | 24 |
| Figure 3.9.  | Air box.....   | 25 |
| Figure 3.10. | Fuel Burette.....  | 26 |
| Figure 4.1.  | Geometrical model of the Heat Recovery Unit.....                 | 30 |
| Figure 4.2.  | Top view of the Heat Recovery Unit.....                          | 30 |
| Figure 4.3.  | Isometric view of arrangement of the tubes.....                  | 31 |
| Figure 4.4.  | Meshing of the Heat Recovery Unit.....                           | 31 |
| Figure 4.5.  | Close up of shell and tubes mesh.....                            | 32 |
| Figure 4.6.  | Close up mesh at the longitudinal mid-section of HRU.....        | 32 |

|   |    |
|---|----|
| Figure 5.1. Variation of Thermic oil temperature with respect to time at a load of 4.4kW during charging of HRU (14 November 2016)..... | 41 |
| Figure 5.2. Variation of $T_e$ , $T_i$ and $T_o$ with respect to time at a load of 4.4kW during charging of HRU (14 November 2016)..... | 42 |
| Figure 5.3. Variation of Thermic oil temperature with respect to time during discharging of HRU (14 November 2016).....                 | 44 |
| Figure 5.4. Variation of $T_i$ and $T_e$ with respect to time during discharging of HRU (14 November 2016).....                         | 44 |
| Figure 5.5. Temperature contour of the HRU model(using Thermic Oil as ESM) during charging.....   | 45 |
| Figure 5.6. Temperature contour at longitudinal mid-section plane of HRU during charging condition (using Thermic Oil as ESM).....      | 46 |
| Figure 5.7. Temperature contour at longitudinal mid-section plane of HRU during discharging condition (using Thermic Oil as ESM).....   | 49 |
| Figure 5.8. Comparison between experimental and simulation results during discharging (using Thermic Oil as ESM).....                   | 50 |
| Figure 5.9. Variation of temperature of Erythritol with respect to time at a load of 4.4kW during charging of HRU.....                  | 52 |
| Figure 5.10. Variation of temperature of Erythritol with respect to time during discharging of HRU.....                                 | 53 |
| Figure 5.11. Temperature contour of the HRU model (using Erythritol as ESM) during charging.....  | 53 |
| Figure 5.12. Temperature contour at longitudinal mid-section plane of HRU during charging condition (with Erythritol as ESM).....       | 55 |
| Figure 5.13. Temperature contour at longitudinal mid-section plane of HRU during discharging condition (with Erythritol as ESM).....    | 57 |

Figure 5.8. Comparison between experimental and simulation results during discharging (using Erythritol as ESM).....58

## LIST OF TABLES

|             |   |    |
|-------------|---|----|
| Table 1.1.  | Temperature from the exhaust gas from various diesel engines.....   | 3  |
| Table 3.1.  | Specification of Kirloskar Diesel Engine.....   | 19 |
| Table 3.2.  | Specification of Electric Dynamometer.....  | 20 |
| Table 4.1.  | Scale of measuring mesh quality.....  | 33 |
| Table 4.2.  | Skewness of mesh.....   | 33 |
| Table 4.3.  | Aspect ratios of mesh.....  | 34 |
| Table 4.4.  | Solver setup.....   | 35 |
| Table 4.5.  | Material used for Case I.....   | 36 |
| Table 4.6.  | Material used for Case II.....  | 36 |
| Table 4.7.  | Boundary conditions for Case I.....   | 36 |
| Table 4.8.  | Boundary conditions for Case II.....  | 37 |
| Table 4.9.  | Solution methods used.....  | 37 |
| Table 4.10. | Under relaxation factors.....   | 38 |
| Table 5.1.  | Variation of Thermic oil temperature with respect to time at a load of 4.4kW during charging of HRU (14 November 2016)..... | 40 |
| Table 5.2.  | Variation of Thermic oil temperature with respect to time during discharging of HRU (14 November 2016).....                 | 43 |
| Table 5.3.  | Comparison between experimental and simulation results during charging (using Thermic oil as ESM).....                      | 49 |
| Table 5.4.  | Comparison between experimental and simulation results during discharging (using Thermic oil as ESM).....                   | 50 |
| Table 5.5.  | Comparison between experimental and simulation results during charging (using Erythritol as ESM).....                       | 57 |
| Table 5.6.  | Comparison between experimental and simulation results during discharging (using Erythritol as ESM).....                    | 58 |
| Table B.1.  | Technical specifications of Shell Heat Transfer Oil S2.....   | 66 |
| Table B.2.  | Technical specifications of Erythritol.....   | 66 |
| Table C.1.  | Different thermocouples and their applications.....   | 67 |

## NOMENCLATURE

### ENGLISH SYMBOLS

| Notation      | Description   | Unit      |
|---------------|---|-----------|
| $v_a$         | Volume flow rate of air                                 | $m^3/s$   |
| $m_a$         | Mass flow rate of air                                   | kg/s      |
| $d_o$         | Diameter of orifice                                     | m         |
| $A_{orifice}$ | Area of orifice   | $m^2$     |
| $C_d$         | Coefficient of discharge of orifice                     | Unit less |
| $h_w$         | Manometric deflection                                   | m         |
| $g$           | Acceleration due to gravity                             | $m^2/s$   |
| $T_e$         | Temperature of exhaust gas at the engine exhaust outlet | K         |
| $T_i$         | Temperature of exhaust gas at the HRU inlet             | K         |
| $T_o$         | Temperature of exhaust gas at the HRU outlet            | K         |
| $u, v, w$     | Velocity in x, y and z directions                       | m/s       |
| $k$           | Fluid thermal conductivity                              | W/mK      |

### GREEK SYMBOLS

| Notation | Description       | Unit      |
|----------|-------------------|-----------|
| $\rho_a$ | Density of air    | $kg/m^3$  |
| $\rho_w$ | Density of water  | $kg/m^3$  |
| $\mu$    | Dynamic Viscosity | Pa.s      |
| $\eta$   | Efficiency        | Unit less |

## LIST OF ABBREVIATIONS

|        |   |
|--------|---|
| CCHP   | Combined cooling heating and power        |
| COP    | Coefficient of performance                |
| WHR    | Waste heat recovery                       |
| LHTESS | Latent heat thermal energy storage system |
| TES    | Thermal energy storage                    |
| VARs   | Vapour absorption refrigeration system    |
| HTF    | Heat transfer fluid                       |
| SHS    | Sensible heat storage                     |
| PCM    | Phase change material                     |
| ORC    | Organic Rankine Cycle                     |
| HRU    | Heat recovery unit                        |
| ESM    | Energy storage material                   |
| TEG    | Thermoelectric generators                 |
| AC     | Air conditioner                           |
| ICE    | Internal combustion engine                |
| CI     | Compression ignition                      |
| HC     | Hydrocarbon                               |
| CFC    | Chloroflourocarbon                        |
| CO     | Carbon monoxide                           |



## **1.1 Waste heat**

Waste heat can be defined as the heat which is generated in a process by way of combustion of fuel or chemical reaction, and then rejected into the environment even though it could be still used for some useful and economic purpose. The essential quality of heat is not the amount but rather its “value”. The strategy to recover this heat depends in part on the temperature of the waste heat gases and the economics involved.

Waste heat can be divided into three categories according to the temperature such as:

- High Temperature Range: Temperature above 650°C.
- Medium Temperature Range: 230 °C - 650 °C.
- Low Temperature Range: below 230 °C.

High and medium temperature range waste heat is mainly released by the furnaces while the low temperature range waste heat is released by devices like condenser, solar flat plate collector etc.

## **1.2 Waste heat recovery**

Waste heat recovery means the collection of heat which is generated as a by-product of the operation of a piece of equipment or machine to fill a desired purpose elsewhere. It is evident that large quantity of hot flue gases is released from boilers, kilns, ovens, furnaces etc. If some of this waste heat could be recovered and reused, a considerable amount of primary fuel could be saved. The energy which is lost in the waste gases cannot be totally recovered. However, much of the heat could be recovered by adopting various measures.

Depending upon the process, waste heat can be virtually rejected at any temperature from that of chilled freezing water to high temperature waste gases from an industrial furnace or kiln. Usually higher the temperature, better the quality of waste heat and more cost effective is the heat recovery. In any study of waste heat recovery, it is absolutely necessary that there should be some use for the recovered heat. Typical examples of use would be preheating of combustion air, space heating, or pre-heating boiler feed water or process water. With high

temperature heat recovery, a cascade system of waste heat recovery may be practiced to ensure that the maximum amount of heat is recovered at the highest potential.

### 1.3 Waste heat recovery in internal combustion engines

Out of the total heat supplied to an internal combustion engine in the form of fuel, approximately 30-40% is converted into useful mechanical work; the remaining heat is expelled to the environment through exhaust gas and engine cooling systems, resulting into entropy rise and serious environmental pollution. So it very important to utilize this waste heat into useful work. The recovery and utilization of waste heat not only conserves fuel but also reduces the amount of waste heat and greenhouse gases dumped into the environment.

Waste heat losses occur both from the equipment inefficiencies and thermodynamic limitations on equipment and processes. For example, let us consider an internal combustion engine converting 30-40% of supplied energy into useful mechanical work. This implies 60-70% of the supplied energy is lost as waste heat. Exhaust gases leaving the engine can have temperatures as high as 400-600°C which means that these gases have high heat content. Figure 1.1 shows the total energy distribution of an internal combustion engine.

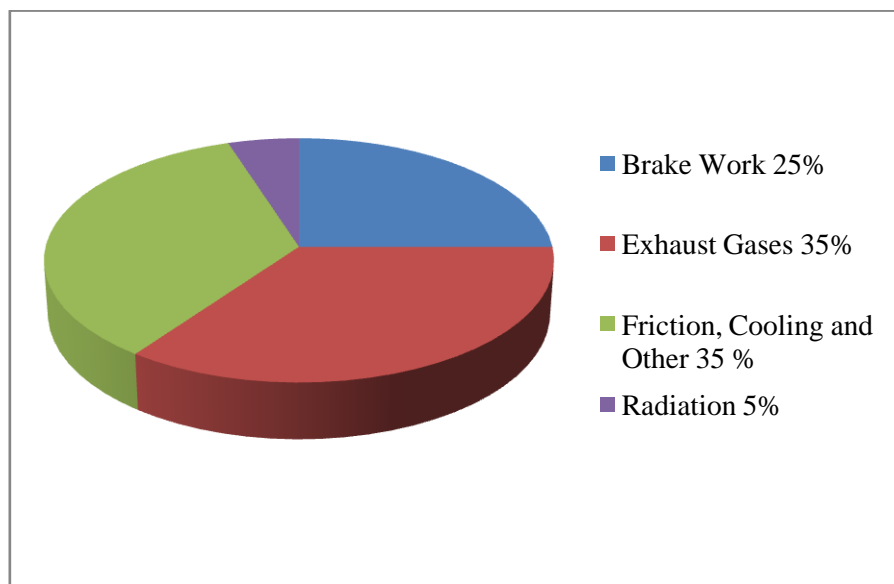


**Figure 1.1: Total fuel energy distribution in I.C engine**

**Table 1.1: Temperature from the exhaust gas from various diesel engines**

| Engine  | Temperature (°C) |
|---|------------------|
| Single cylinder four stroke diesel Engine                       | 450-500          |
| Four cylinder four stroke diesel engine (Tata Indica)           | 400-450          |
| Six cylinder four stroke diesel engine (Tata truck)             | 330-340          |
| Four cylinder four stroke diesel engine (Mahindra Arjun 605 DI) | 300-320          |
| Genset (Kirloskar) at power 198 hp                              | 380-390          |
| Genset (Cummins) at power 200 hp                                | 390-400          |

## 1.4 Advantages and disadvantages of waste heat recovery from I.C. engines

### 1.4.1 Advantages of waste heat recovery

Advantages of waste heat recovery from I.C engines can be broadly classified into two categories:

#### Direct benefits:

Waste heat recovery from I.C. Engines enhances the combustion process efficiency which is reflected by the reduction in utility consumption and process cost.

#### Indirect benefits:

- *Reduction in pollution:* Recovery of waste heat reduces emission of toxic combustible wastes, such as carbon monoxide CO, hydrocarbons (HC), nitrogen oxides (NO<sub>x</sub>), particulate matters etc.
- *Reduction in equipment sizes:* The recovery of waste heat from I.C. engines reduces the fuel consumption, which leads to the reduction in flue gases produced. This eventually results in the reduction of equipment size.
- *Reduction in auxiliary energy consumption:* Reduction in equipment sizes gives additional benefits in the form of reduction in auxiliary energy consumption.

## 1.4.2 Disadvantages of waste heat recovery

- *Increase in backpressure:* With the installation of a waste heat recovery system in a vehicle exhaust system, the backpressure of the engine may increase resulting in reduced engine volumetric efficiency and thus reduced fuel conversion efficiency.
- *Increase in weight:* The added weight of waste heat recovery system on an automobile will negatively affect the total gain in fuel economy.
- *Maintenance of equipment:* Additional equipment added to waste heat recovery requires additional maintenance cost.
- *Capital cost:* Sometimes capital cost to implement a waste heat recovery system may be more than the benefit gained in heat recovered.

## 1.5 Methods of waste heat recovery

### 1.5.1 Thermoelectric generation

Thermoelectric Generator (TEG) is a device which converts thermal energy from different temperature gradients existing between hot and cold ends of a semiconductor into electric energy. In regards with the applicability of TEG in modern engines, the ability of ICEs to convert fuel into useful power can be increased through the utilization of the mentioned device. Advantages of TEG include free maintenance, silent operation, high reliability and involving no moving and complex mechanical parts. Disadvantages include low efficiency and high cost.

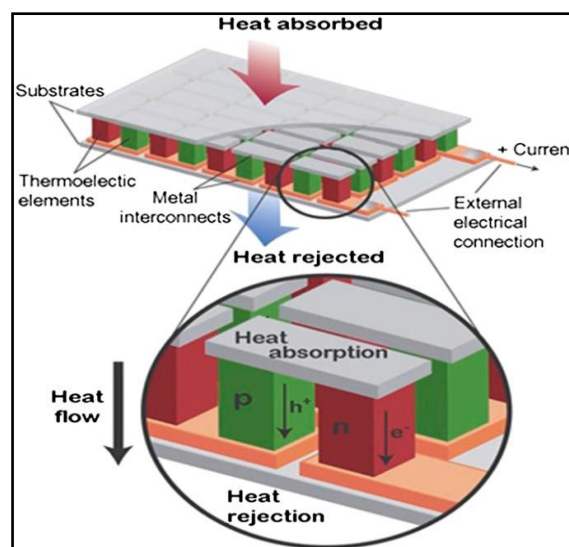


Figure 1.2: Schematic of a typical TEG

### 1.5.2 Organic Rankine Cycle (ORC)

An organic Rankine Cycle (ORC) consists of organic fluid (i.e., dry or isentropic) as the working fluid, a pump to circulate the working fluid (increase in pressure), an evaporator /boiler to absorb exhaust heat energy, an expansion machine to release power by bringing the fluid to a lower pressure level (organic vapor expands in the turbine to produce mechanical energy), a condenser to release the heat from the fluid before starting the whole cycle again. It can be said that the efficiency of the cycle is greatly dependent on the selection of the working fluid. An organic Rankine cycle uses isentropic organic fluid due to their low heat of vaporization and they do not need to be superheated to increase their recovery.

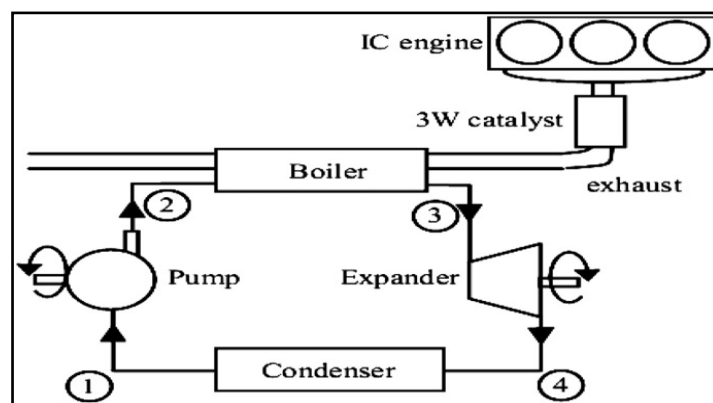


Figure 1.3: Layout of the WHR Organic Rankine Cycle

### 1.5.3 Turbocharging

In Turbocharging method engine exhaust energy is used to drive the turbocharger turbine and this turbine is coupled with the turbocharger compressor which raises the inlet fluid density prior to entry to each engine cylinder and in turn provides boost to the inlet air (or mixture).

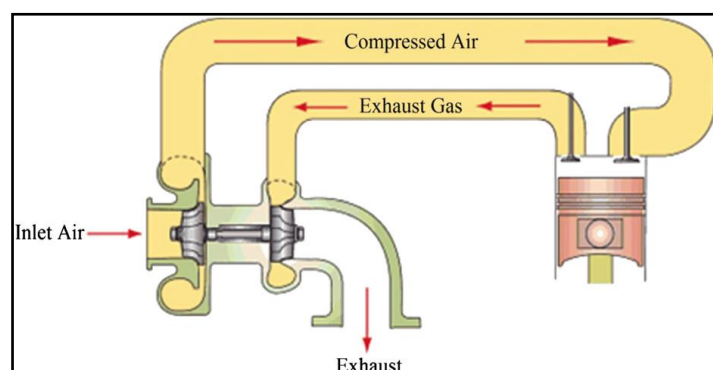


Fig 1.4: Typical turbocharger with compressor wheel and turbine

## 1.5.4 Turbocompounding

Turbocompounding of an engine refers to the use of a turbine to recover energy from the exhaust system of an internal combustion engine and reintroduce that energy back into the engine. It increases thermal efficiency and reduces toxic emissions of an engine. Turbocompounding are classified as:

### Mechanical turbocompounding

In Mechanical Turbocompounding, the waste energy recovered from exhaust gases is converted into kinetic energy and turbine output shaft is connected to crankshaft through a gear train for speed reduction so this energy is added to the engine torque through system of shafts, gears and fluid couplings.

With Mechanical Turbocompounding high power density (more power for a given displacement) and better fuel consumption is obtained. In this technique exhaust manifold pressure is increased above intake manifold pressure. Higher EGR-flow can be achieved more easily to facilitate low  $\text{NO}_x$  emissions

Mechanical Turbocompounding has negative effect at low loads and idling speeds and system work as an energy consumer, thus pulling down the average BSFC. Various researchers reported that the improvement in BSFC of a heavy duty diesel can be obtained in the range of 4-6% at full load and ~2-3% at part load condition [5]. It also has disadvantage that gear train, fluid coupling, and power turbine add weight, complexity and cost.

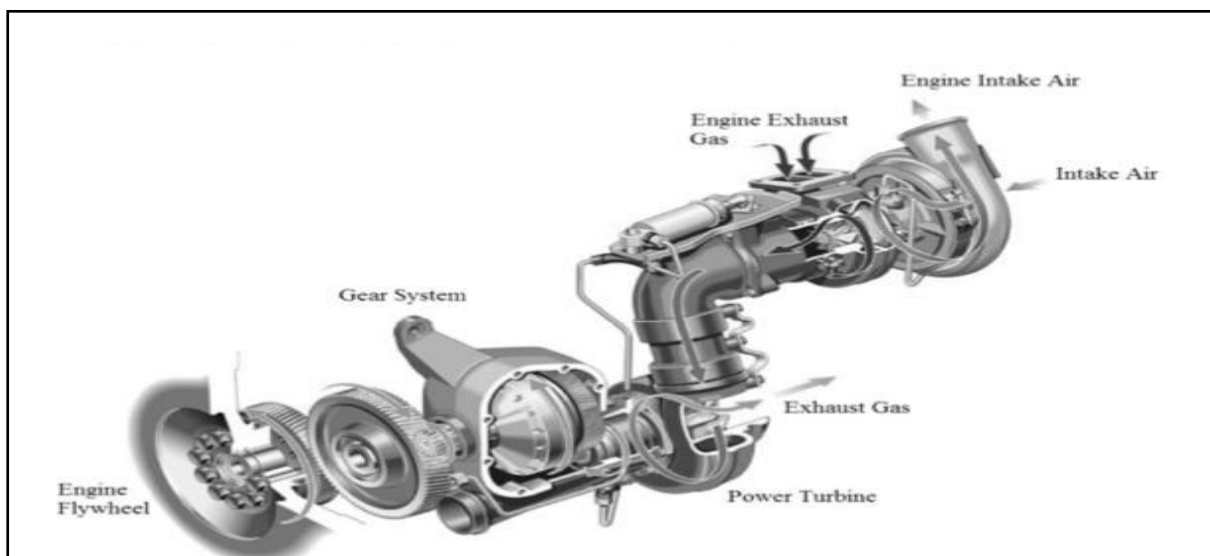


Figure 1.5: Layout of mechanical turbocompounding

## Electrical turbocompounding

In Electrical Turbocompounding instead of driving mechanically an electrical generator is connected to the turbine output shaft. The energy recovered from exhaust gases is converted into electrical power and then transmitted to the engine by a power electronics module.

It has advantage over Mechanical Turbocompounding as it increases ability to control turbine power output and speed independently of engine load and speed. It gives better performance and reduces the emissions.

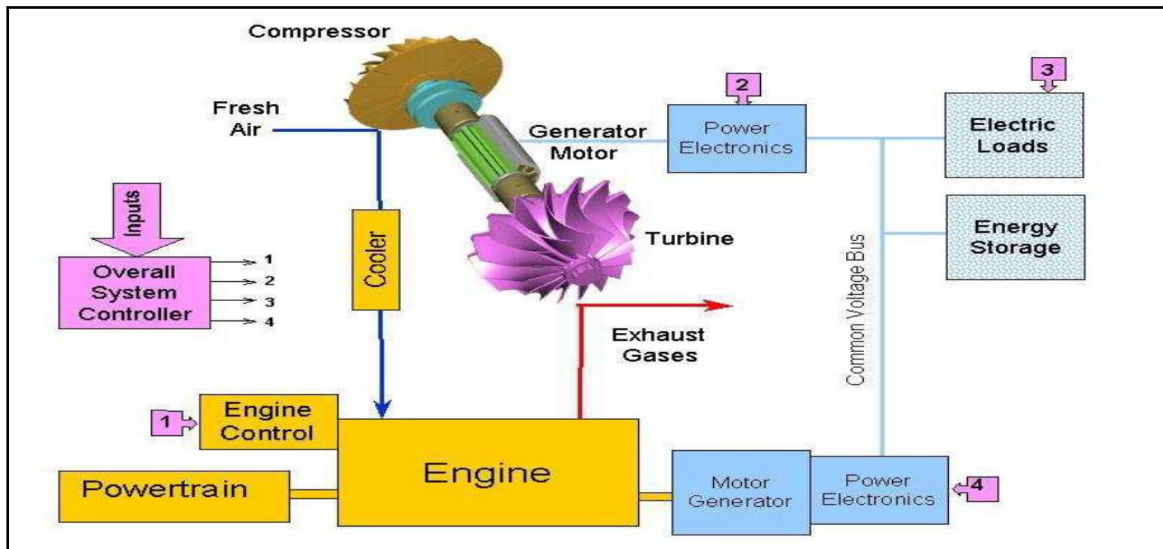


Figure 1.6: Electric turbocompounding system

### 1.5.5 Six-stroke internal combustion engine

In six-stroke internal combustion engine extra two strokes are added to produce higher efficiency and reduced emissions. The basic concept is similar to four stroke engine cycle.

In the proposed six-stroke cycle there are two methods of operation:

- In the first method water is injected after complete finish of exhaust stroke. But when the water is injected into the cylinder it produces impingement on the combustion chamber surfaces, because hot combustion chamber surfaces are utilized as primary heat source.
- The second method is by trapping and recompressing some of the exhaust gases from the fourth piston stroke, followed by a water injection and expansion of the resulting steam/exhaust mixture.

## **1.6 Outline of thesis**

### **Chapter 1: Introduction**

The first chapter presents an overview of feasible waste heat recovery technologies for internal combustion engines like Thermoelectric Generators (TEG), Organic Rankine Cycle (ORC), Turbocharger, Six-stroke internal combustion engine etc. The various advantages and disadvantages of waste heat recovery technologies are also highlighted in this chapter.

### **Chapter 2: Literature Review**

In this chapter an exhaustive study regarding the various Waste Heat Recovery technologies have been done. It also includes research gap based on the literature survey and objectives of the research.

### **Chapter 3: Experimental Setup and Procedure**

It covers the experimental setup describing the different components and measuring instruments used in the study. It also includes the detailed plan or procedure for conducting the experiments.

### **Chapter 4: CFD Modeling and Simulation**

In this chapter a detailed explanation of the steps involved in geometrical modeling and subsequent meshing of a Heat Recovery Unit has been provided. The steps involved in simulation of the developed model of HRU are also discussed in this chapter.

### **Chapter 5: Results and Discussions**

The results obtained from experimental analysis and simulation have been summarized and discussed in this chapter.

### **Chapter 6: Conclusion**

The seventh and last chapter reports the conclusions drawn from the study and future scope of work.



A detailed literature is available on the various technologies of recovering waste heat from the internal combustion engines. Researchers around the world are carrying out various experimental, numerical and computer simulation work in this field so that maximum amount of the waste heat could be harvested and utilized. The chapter presents an overview on various research materials studied for the development of this project. A detailed discussion of different experimental, numerical, theoretical and computational studies on the various technologies of waste heat recovery from internal combustion engines has been presented in this chapter.

### 2.1 Experimental investigations

**Kim et al., 2016 [1]** carried out an experimental investigation on the waste heat recovery performance of a thermoelectric generator (TEG). In the experimental setup, forty customized thermoelectric modules (TEMs) were installed on the upper and lower sides of a rectangular exhaust channel in a 4 x 5 arrangement. To create a temperature difference across each TEM, water at ambient temperature was supplied from a cooling tower. A turbocharged six- cylinder diesel engine was used as the heat source and the engine was operated under various conditions. Inorder to determine the effect of the exhaust gas flow rate on TEG power output, three engine rotation speeds- 1000, 1500 and 2000 rpm were employed. By changing the engine load, the temperature of the exhaust gas was varied. From the experimental results, a contour showing the power output of TEG as a function of engine load and speed was obtained. It has been observed from the contour map that the power output of the TEG increases with engine load or speed. The maximum power obtained was approximately 119 W at 2000 rpm with a BMEP of 0.6 MPa, while the maximum energy conversion efficiency was around 2.8 %. Under all engine operation condition, the pressure drop across the TEG was experimentally found to be 0.45-1.46 kPa.

**Kim et al., 2016 [2]** developed a highly efficient single-loop Organic Rankine Cycle (ORC) to recover waste heat from the engine of a gasoline vehicle. In this paper, the performances of several conventional single loop ORC systems for engine waste heat recovery has been compared, and their limitations to realizing maximum power were considered. After that, a novel

single loop ORC system has been proposed that maximizes power by effectively utilizing waste heat from both low-temperature sources (coolant) and high-temperature sources (exhaust gas) in an I.C. engine. The novel single-loop system produced approximately 20% additional power from engine WHR when operating under the target engine conditions.

**Johar et al., 2016 [3]** developed a latent heat thermal energy storage system (LHTESS) and integrated with a stationary CI engine. The LHTESS is a shell and tube type heat exchanger having 346mm diameter and 420 mm height with 45 number of tubes of 18 mm diameter. The LHTESS was developed to store thermal which was recovered from the hot exhaust gases of the engine and Erythritol was used a phase change material. The performance of the engine and performance parameters the thermal energy storage system such as amount of heat stored, charging efficiency etc. were evaluated. From the experimental results, it was observed that there was a slight decrease in the engine performance when the LHTESS was integrated to the engine. But the energy which was recovered from the LHTESS was significantly high. The maximum charging efficiency, energy recovery efficiency and percentage energy saved at a load of 4.4 kW was 69.53 %, 38 % and 11.33% respectively.

**Wang et al., 2015 [4]** carried out experimental analysis with a CCHP (Combined cooling heating power) system in a dual source powered mixed effect AC. The performance of this mixed effect AC under both waste heat mode and solar mode were tested and compared. In waste heat mode, the AC was powered by exhaust gas waste heat and hot water from an I.C. Engine. While in solar mode, the AC was powered by hot water producing from a solar thermal collector matrix, and its refrigeration performance was tested on a selected day to study the operation characteristics. Test results showed that the COP in waste heat mode was 0.91 while in solar mode it was 0.6. Comparison the results, it was found that waste heat mode was not always better than solar mode and vice versa. In terms of primary energy consumption, solar mode was found to be better than waste heat mode when the part load ratio of ICE was below 0.62.

**Goyal et al., 2015 [5]** carried out an experimental investigation of CI engine operated micro-cogeneration system for power and space cooling. In the cogeneration system, in addition to the electricity generated from the genset, waste heat recovered from the exhaust of diesel engine was used to drive a combination of four units of Electrolux vapour absorption (VA) system for space cooling. The capacity and heat input of each unit of VA system was 51 Litre and 95 W

respectively. For space air conditioning, a cabin of 900 mm width, 1500 length and 1800 mm height made of plywood was fabricated. A drop of 5°C temperature was obtained in the cabin at full engine load about 6 hours after system start up. The reduction of carbon dioxide emission in kg per kWh of useful energy output was 19.49% compared to that of single generation at full load. The decrease in specific fuel consumption in case of cogeneration system compared to that in single generation was 2.95% at full load. The test results showed that micro capacity (3.7 kW) stationary single cylinder diesel engine could be successfully modified to produce power and space cooling simultaneously.

**Wang and Wu, 2015 [6]** developed a mixed effect absorption chiller (AC) which recover heat both from the jacket water and exhaust gas. In the high pressure generator, heat is supplied by the exhaust gas from IC engine while in the low pressure generator heat is supplied from jacket water. The thermodynamic characteristics and off design performance are simulated. After considering the thermodynamic constraints, the start point temperature in the low pressure generator is found out to be 77 °C or lower. For 16 kW ICE, the cooling output had reached 34.4kW with COP of 0.96 and the exergy efficiency 0.186.

**Fu et al., 2013 [7]** developed a noble approach for exhaust heat recovery to improve the fuel efficiency of IC engine. An open organic Rankine cycle system with methanol as working medium is integrated to IC engine exhaust pipe for waste heat recovery. In the bottom cycle, methanol first undergoes dissociation and expansion process. Then it is directed back to IC engine as fuel. As the external bottom cycle and main cycle of IC engine are integrated together, this scheme forms a combined thermodynamic cycle. Later this concept was applied to a turbocharged engine, and the corresponding simulation models were created for both the IC engine main cycle and external bottom cycle. By parametric analyses, the energy saving potential of this combined cycle was estimated. It was found that the compared to the methanol vapor engine the IC engine in-cylinder efficiency has increased by 1.4-2.1 percentage points under full load. Further, it was also found that the external bottom cycle can increase the efficiency of the fuel by 3.9-5.2 percentage points at 30 bar working pressure.

**Fu et al., 2012 [8]** developed an open steam power cycle which uses waste heat from the exhaust of I.C. Engine. The concept of bottom cycle was designed on a four cylinder naturally aspirated I.C. engine. Three cylinders were used as ignition cylinder and one cylinder was used for steam expansion. The I.C. engine exhaust pipe was coupled with a Rankine steam cycle system which

used the high temperature of the exhaust gas to generate steam. The steam was then injected into the steam expansion cylinder where it expanded. From the experimental results of this research it has been found that the exhaust gas energy is mainly limited by exhaust gas temperature. The maximum power of the bottom cycle was found to be 19.2 kW and there was 6.3 % improvement in thermal efficiency of the I.C. engine at 6000 rpm. This study has proved that the novel bottom cycle concept has a great potential for energy saving and emission reduction of I.C. engine.

**Christopher et al., 2012 [9]** carried out experimental analysis on a single effect ammonia-water absorption system which was driven by the heat rejected from a diesel engine. The waste heat is recovered using an heat exchanger and then it is delivered to the desorber by a heat transfer fluid loop. The absorber and condenser are coupled in parallel to an ambient heat exchanger for heat rejection. A thermodynamic model was developed for a baseline cooling capacity of 2kW and a detailed parametric study of the optimized system was conducted for both cooling and heating mode operation over a range of operating conditions. These parametric investigations showed that degradation of system performance can be limited, and improved COPs can be achieved by adjusting the coupling fluid temperature with the variation of ambient temperature. With the variation of return air temperature, the system was able to provide the 2kW design cooling capacity for the entire range of ambient temperature.

**Pandiyarajan et al., 2011 [10]** carried out a thermodynamic energy and exergy analysis on the experimental setup consisting of a finned shell and tube heat exchanger and a thermal energy storage tank (TES) with paraffin as the phase change material for waste heat recovery from the exhaust of a diesel engine. Castor oil is used as the heat transfer fluid (HTF) to extract heat from the exhaust gas, and it also serves as a sensible heat storage (SHS) medium. Experimental investigations have been carried out for the charging process of the PCM in the TES tank for various engine load conditions. Through this analysis the sources of losses in useful energy is identified within the components of the system considered. It also provides a more realistic and meaningful assessment than the conventional energy analysis. The energy and exergy balance for the overall system is quantified and illustrated, using energy and exergy flow diagrams.

**AlQdah, 2011 [12]** carried out an experimental study of aqua-ammonia absorption system used for automobile air conditioning system using waste heat from a diesel engine. The estimated

cooling load for the automobile found to be within acceptable ranges which are about 1.37 ton refrigeration. The obtained results showed that the COP values were directly proportional with increasing generator and evaporator temperatures but decrease with increasing condenser and absorber temperatures. The COP value was found in the range of 0.85 and 1.04.

The main components of the absorption refrigeration cycle were designed and fabricated for optimal performance. The system was found to be applicable and ready to produce the required conditioning effect without any additional load to the engine. The present system decreases vehicle operating costs and environmental pollution caused by the heating system.

**Manzela et al., 2010 [11]** performed an experimental study on an ammonia-water refrigeration system using waste heat from an IC engine exhaust. The availability of exhaust gas energy and the impact of the engine performance due to the integration of vapour absorption refrigeration system, and power economy were evaluated. The engine was tested for 25 %, 50 %, 75% and wide open throttle valve. It was seen that the refrigerator had reached a steady state temperature between 4°C and 13°C about 3 hour after system start up, depending upon the throttle valve opening. The calculated exhaust gas energy availability suggests the cooling capacity can be highly improved for a dedicated system. The exhaust hydrocarbon emissions were found to be higher when the refrigeration system was integrated with the engine, but carbon monoxide emissions were reduced, while carbon dioxide concentration remained practically unaltered.

**Khatri et al., 2010 [13]** developed a micro-trigeneration system based on a CI engine and carried out experimental investigations to evaluate the performance and emissions of the original single generation system and the trigeneration system developed. From the test results it has been found that the total thermal efficiency of trigeneration system reached to 86.2% at full load while it was only 33.7% for the original single generation system, at the same load. The CO<sub>2</sub> emission from the trigeneration system was 0.1211 kg/kWh compared to 0.308 kg/kWh from the single generation at full load. The reduction of CO<sub>2</sub> emission in kg per unit (kWh) of useful energy output is 60.71% as compared to that of single generation at full load.

The objective of this study was to investigate the feasibility to develop a Micro-Trigeneration system based on small capacity agricultural engine (3.7kW) which can serve a small residential home of a village in a developing country like India. The waste heat from the engine cooling

system and engine exhaust system has been utilized to generate hot water through a heat exchanger and cooling or refrigeration through a vapor absorption refrigerator.

**Jiangzhou et al., 2005 [14]** developed an adsorption air conditioning system used in internal combustion engine locomotive driver cabin. The system consists of an adsorber and a cold storage evaporator driven by the engine exhaust gas waste heat, and employs zeolite-water as working pair. The mean refrigeration power obtained from the prototype system was 5kW, and the chilled air temperature was 18°C. The authors described the system was simple in structure, reliable in operation, and convenient to control, meeting the demands for air conditioning of the locomotive driver cabin.

## 2.2 Theoretical and simulation studies

**Temizer and İlkilic, 2016 [15]** performed a study on the thermoelectric generator system used in diesel engine. They developed a prototype for the working principle suitable to the thermoelectric generator system. The exhaust systems of diesel engine is used and benefited from the exhaust gas to heat the surface. In addition to that, thermoelectric cooling system is used for the required cooling effect under different temperatures. For experimental analysis diesel engines are used in five different engine speeds and two different engine loads for each speed levels. Electric connection of the 40 piece thermoelectric modules mounted on the octagon structure made from Aluminium 6061 material is made in series. The performance of TEG systems has been analyzed in terms of changing speed and load of the engine. The temperature and flow analysis was performed with the assistance of Fluent programme in the Ansys Workbench 12.0

**Bhore et al., 2016 [16]** developed and tested a vapor absorption refrigeration system by utilizing coolant and exhaust waste heat. The performance of the system was also analyzed in EES (Engineering Equation Solver) for various working conditions. It was seen that a large amount of low grade was available (3.275kW), can be recovered from the exhaust. Also it was found that, COP of the system decreased with the increase in generator and condenser temperature. Theoretically it was estimated to have COP of about 1.517. A 10 °C temperature reduction was observed at the evaporator and it is the refrigeration effect produced using the waste heat

**Wang et al., 2015 [17]** studied the thermal-hydraulic characteristics of an ORC evaporator using a CFD method. The authors derived a 3D numerical model of the fin and tube evaporator and

specified the boundary conditions according to the data obtained by the engine test. From the simulation results it was observed that the exhaust on the shell side flows mainly parallel with the fin layers. It was also observed that alternating high and low temperatures appeared on the middle planes of the adjacent tube rows. The shape of the front and rear end parts which connects the main body to the exhaust pipes are important factors to be considered on the flow field. Further, it was observed that the maximum exhaust pressure decrease in the fin and tube evaporator was less significantly than the backpressure limit which was required by the engine exhaust pipe.

**Dong et al., 2015 [18]** carried out experimental analysis by integrating a refrigeration and power system using Organic Rankine cycle (ORC) and solid sorption technology into internal combustion engines. A one dimensional engine model was coded using WAVE to evaluate the waste heat quantity of a medium duty diesel engine. The recoverable waste heat from the coolant and exhaust system has been analyzed under engine overall operational region. Based on these results, the working conditions of a cogeneration were designed and the performance of the cogeneration was evaluated throughout the engine operating region. The system has the potential to improve the overall efficiency of the ICE from 40% to 47%.

**S. Lakshmi, 2013 [19]** analyzed the use of energy from the exhaust gas of internal combustion engine to power a vapour absorption refrigeration system to air condition an ordinary passenger car. A preheater is employed to utilize the cooling water heat for preheating the  $\text{NH}_3$  solution flowing from absorber to generator. Thermal analysis of evaporator and condenser is done in ANSYS for aluminum alloy 204 and copper. By observing the analysis results, it was found that thermal flux is more for aluminum alloy 204 than copper for both condenser and evaporator. So it would be preferable to use aluminum alloy 204.

**Saidur et al., 2012 [20]** reviewed the latest developments and technologies on WHR of exhaust gas from I.C. engines. These include Organic Rankine Cycle (ORC), thermoelectric generators (TEG), six-stroke cycle I.C. engine and new developments on turbocharger technology. The author also studied about the potential of energy savings and performances of those technologies. It is evident that the current worldwide trend of increasing energy demand in the transportation sector is one of the many factors that is responsible for the growing share of fossil fuel usage and indirectly leads to the release of harmful greenhouse gases (GHG) emissions. The author further

stated that with the latest findings on exhaust heat recovery to enhance the efficiency of ICEs, world energy demand on the depleting fossil fuel reserves would be reduced and hence the impact of global warming due to the GHG emissions would reduce subsequently.

**Wang et al., 2011 [21]** reviewed relevant researches on the various methods of waste heat recovery from the I.C. engines. According to the author, Rankine cycle has been the most favorite basic working cycle for thermodynamic exhaust heat recovery systems. Based on the cycle, various system configurations have been investigated. The authors also stated that exhaust heat recovery based on thermoelectric (TE) and thermal fluid systems have been explored widely many new technologies have been developed in the past decade.

**Li and Wu, 2009 [22]** developed and constructed a micro CCHP system which is based on a two bed silica gel-water adsorption chiller. By using results from the numerical simulation the authors found that the cooling capacity and the coefficient of performance (COP) of the chiller were significantly influenced by the average value and variation of electric load, as well as the average value of cooling load. The authors recommended the use of water tank in order to get better performance of the chiller and acceptable start-up time. Also the use of a cold accumulator for higher performance and system security was recommended. The water tank has drastic effect on the chiller performance. To obtain better chiller performance, the water tank should be adopted when the electric load is low or its variation rate is positive. Again, the water should not be used when the electric load is high or its variation is negative. Further, a cold accumulator should be adopted to get better performance and acceptable start-up time.

**Talbi and Agnew, 2002 [23]** analyzed the theoretical performance of four different configurations of a turbocharged diesel engine and absorption refrigeration unit combination when it was operating in an ambient day temperature of 35°C. The simulation was performed using a well known programme commonly used for engine performance prediction, "SPICE". They examined the interfacing of the turbocharged diesel engine with an absorption refrigeration unit and estimated the performance enhancement. The influence of the cycle configuration and performance parameters on the performance of the engine operating as a power supply with an auxiliary air conditioning plant was examined. It was demonstrated that a pre and intercooled turbocharger engine configuration cycle offers a lot of benefits in terms of SFC, efficiency and output for the diesel cycle performance.



**Meunier, 2001 [24]** discussed adsorption air conditioning for automobiles as a very challenging possibility for adsorption cooling. The author states that car air conditioning is an ideal solution for sorption systems to be competitive from global warming point of view, even with low coefficient of performances (COP). The technological difficulties are on the need for light and compact units, requiring efficiency improvement and heat transfer intensification the absorbers to reduce the size and weight of the units.

**Koehler et al., 1997 [25]** developed and tested a prototype of absorption for truck refrigeration using heat from the exhaust gas. The refrigeration cycle was simulated by a computer model and validated by test data. The recoverable energy from the exhaust gas was analyzed the truck driving conditions at city traffic, mountain roads and flat roads. The prototype showed a coefficient of performance of about 27 %, but system simulation showed that it could be improved nearly by double.

### **2.3 Research gaps based on the literature survey**

On the basis of detailed review of the literatures, we can say that there are large potentials of energy savings through the waste heat. The waste heat recovery from exhaust gas and conversion into mechanical power is possible with the help of Rankine, Brayton thermodynamic cycles, mechanical turbo-compounding and vapour absorption refrigeration system. These are the different techniques to recover maximum possible waste heat energy and a lot of research work has been on these techniques. But still there are some areas which require special attention for further research studies:

- At low load and idling speed mechanical turbo-compounding system are energy consumer. So mechanical turbo-compounding even though considered as standard technology deserves further research to examine the potential of exhaust energy recovery.
- Due to easy and steady operating conditions for stationary engines it seems that the heat exchanger integrated stationary engines have a great potential of energy saving. So more research is required in this area because with the help of heat exchangers there is a great chance to recover the exhaust waste heat of stationary IC engines at every load and every speed of the engine.

- In most of the research work, the Thermal Energy Storage (TES) system has been predominantly used for harvesting solar energy. But there is great potential of energy saving by the application of TES system in IC engines.
- Limited research work has been done in the field of small capacity CI engine operated waste heat recovery systems. There is need to study waste heat recovery systems with small capacity C.I. engines.
- Very few simulation and experimental studies are available in the literature related to integration of thermal storage with Cogeneration and Trigeration system.

## **2.4 Objectives of the present research**

- To develop a simulation model of the **Heat Recovery Unit (HRU)** using Ansys-Fluent.
- To validate the developed model of the HRU with the experimental results obtained using various thermal energy storage medium.

## EXPERIMENTAL SET-UP AND PROCEDURE

### 3.1 Diesel engine used for heat recovery

Kirloskar make single cylinder air cooled engine as shown in figure 3.1 is used for the present experimental investigation. The technical specifications of the engine are given in table 3.1.



**Figure 3.1: Kirloskar Diesel Engine coupled with Electrical Dynamometer**

**Table 3.1: Specification of Kirloskar Diesel Engine**

| Technical Specification | Description          |
|-------------------------|----------------------|
| Engine type             | Kirloskar Oil Engine |
| Engine Coolant System   | Air Cooled           |
| No. of cylinders        | 1                    |
| Bore x Stroke (mm)      | 87.5 x 110           |
| Compression Ratio       | 17.5:1               |
| Rated Output            | 6 HP, 4.4 kW         |

|   |       |
|---|-------|
| <b>Rated Speed (RPM)</b>                  | 1500  |
| <b>Specific Fuel Consumption (kg/kWh)</b> | 0.252 |
| <b>Fuel Tank Capacity</b>                 | 6.5   |

### 3.2 Dynamometer

Power- star make electric dynamometer is coupled to the engine for measuring torque. It consists of an alternator to which electric bulbs are connected to load the engine. The specifications of the dynamometer used are given in table 3.2

**Table 3.2: Specifications of Electric Dynamometer**

| <b>Technical Specifications</b> | <b>Description</b> |
|---------------------------------|--------------------|
| <b>Model</b>                    | KBM105             |
| <b>Current</b>                  | 21.7 A             |
| <b>Voltage</b>                  | 230 V              |
| <b>Frequency</b>                | 50 Hz              |
| <b>RPM</b>                      | 1500               |
| <b>PF</b>                       | 1.0                |
| <b>kVA</b>                      | 5                  |

### 3.3 Heat recovery unit

The Heat Recovery Unit is a finned shell and tube heat exchanger which extracts heat from the exhaust of a stationary C.I. engine. In this shell and tube type heat exchanger, cylindrical shell was made of mild steel with diameter 346 mm and height of 420 mm. 45 numbers of tubes of diameter 18 mm were fixed in the shell. Four numbers of longitudinal fins were attached to each tube at equal intervals. The shell was insulated with layer of glass wool and a layer of Plaster of Paris.

The tank has inlet and outlet (for exhaust gas) as diverging and converging sections respectively. Diverging section was used at the bottom side of tank to expand the exhaust gas for better heat transfer between exhaust gas and tubes. Converging section was used at the top of the bed to allow easy escape of the exhaust gas. The photographic view of the finned shell and tube heat exchanger with insulation, converging section & diverging section and tube with fins are shown in Figure 3.2, 3.3, 3.4 and 3.5 respectively.



**Figure 3.2: Photographic view of the HRU**



**Figure 3.3: HRU with insulation of glasswool**



**Figure 3.4: Converging and diverging section**



Figure 3.5: Tube with fins.

### 3.4 Development of experimental set-up

The experimental set up consists of a single cylinder, four stroke, air cooled, Kirloskar make diesel engine coupled to an electrical dynamometer, integrated with a Heat Recovery Unit. Burette meter was used to measure the mass flow rate of fuel; Air box was used to measure the mass flow rate of air and K-type (Cr/Al) thermocouples was used to measure temperatures at various places in the Heat Recovery Unit. Figure 3.6 shows the pictorial view of experimental set up while figure 3.7 shows the position of thermocouples.

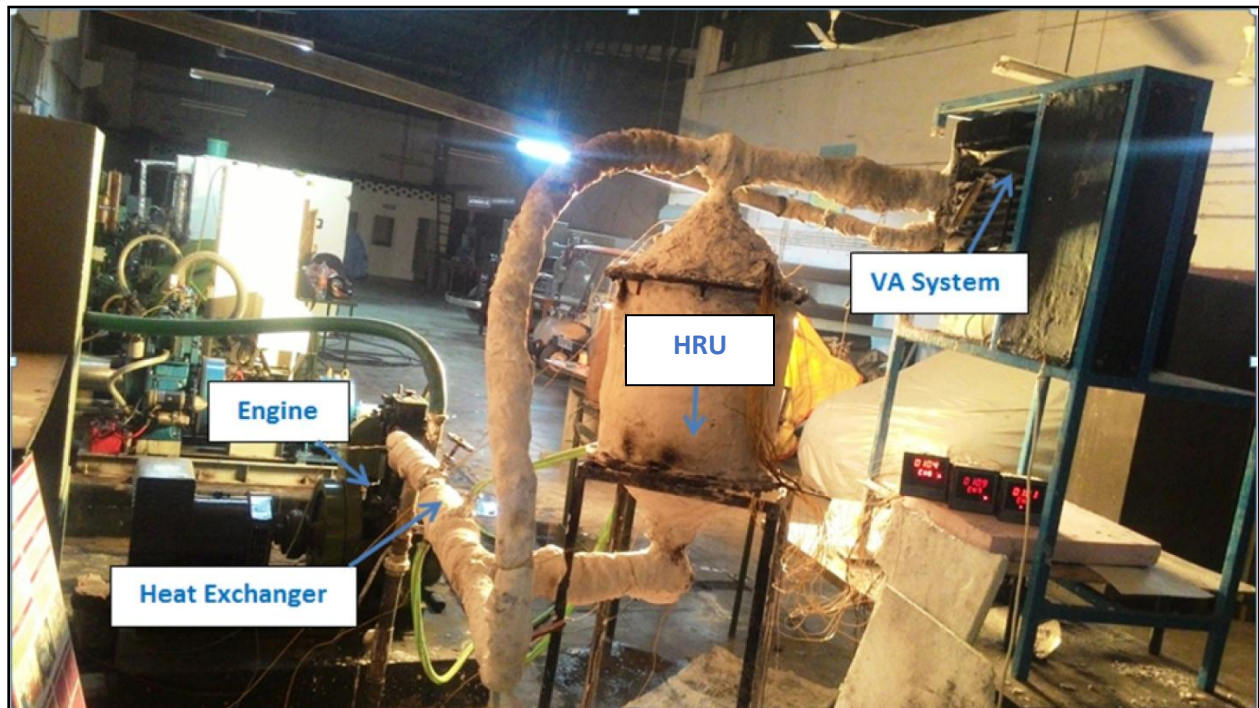
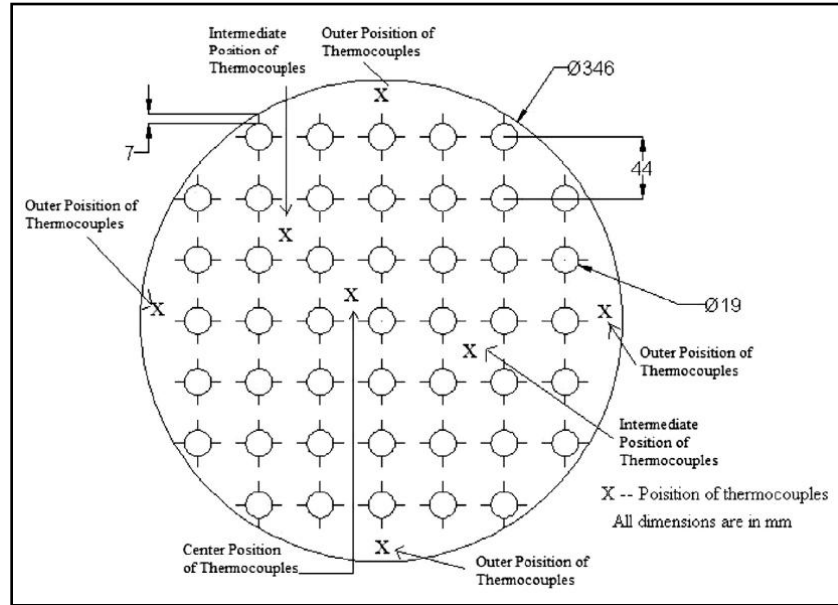


Figure 3.6: Pictorial view of the experimental set-up.



**Figure 3.7: Position of tubes and thermocouples in tank.**

### 3.5 Procedure of experiment

The experiment was carried out using two thermal energy storage materials in the Heat Recovery Unit:

- Phase Change Material : Erythritol ( $C_4H_{10}O_4$ )
- Thermic Oil: Shell Heat Transfer Oil S2

Experiment was carried out in two stages. First stage was charging of HRU and second stage was discharging of HRU. In the first stage, initially the inlet valve to the HRU was closed to obtain the steady state, and then on the accomplishment of the same, inlet valve to the HRU was opened and the bypass valve was closed. Hence, the exhaust gas was passed through the HRU and temperatures at engine exhaust, HRU inlet and outlet, temperatures of the energy storage material at locations were taken at every 5 min interval.

In the second stage (discharging), the engine was kept off and an air blower was used to blow air from the bottom of HRU and hot air was obtained at the top of HRU. The temperatures at various locations of the HRU were noted down again. The discharging process is shown in figure 3.8.



**Figure 3.8: Discharging of HRU**

### **3.6 Heat recovery unit insulation**

In the Heat Recovery Unit surface temperature is very high in comparison to the ambient temperature. As a result of this a large amount of useful heat is radiated away in the absence of insulating materials. A well insulated heat exchanger is highly efficient in comparison to without insulated heat exchanger. To prevent these energy losses from HRU, insulation is the most primary requirement.

We select glass wool and plaster of Paris as insulating material as it has low thermal conductivity and very good fire resistant property.

### **3.7 Air flow measurement**

Air flow to the engine was measured with the help of an Air box as shown in figure 3.9. Air box has orifice of diameter 20 mm having a coefficient of discharge 0.6 was fitted at the entrance on one of the side walls. The outlet was at the bottom through which it was connected to the air filter mounted on the engine. Pressure inside the air box remained less than atmospheric pressure during operation which was measured with the help of a manometer mounted on one of the side



walls. The amount of air induced per second or volume flow rate of air was obtained with the help of the following relation:

$$v_a = C_d \times A_{\text{orifice}} \times \left[ \frac{2gh_w \rho_w}{\rho_a} \right]^{1/2}$$

Where,

$v_a$  is the volume flow rate of air ( $\text{m}^3/\text{s}$ )

$C_d$  is the discharge coefficient of orifice;  $C_d = 0.6$

Diameter of orifice ( $d_0$ ) = **20 mm**,  $A_{\text{orifice}} = \pi d_0^2/4 = \mathbf{0.00031415 \text{ (m}^2\text{)}}$

$h_w$  = Manometric deflection (m),  $\rho_w$  = Density of water ( $1000 \text{ kg/m}^3$ )

$\rho_a$  = Density of air (in  $\text{kg/m}^3$ )

Mass flow rate of the air can be calculated by following equation:

$$\text{Mass flow rate of air} = (\text{Volumetric flow rate}) \times (\text{Density of Air})$$



**Figure 3.9: Air box**

### 3.8 Fuel flow measurement

Burette method was used to measure the volumetric flow rate of the fuel. A glass burette having marks was connected to fuel tank and the engine through a Tee valve which is shown in Figure 3.10. The time taken by the engine to consume a fixed volume of fuel was measured with the help of stopwatch. For calculating the mass flow rate of fuel, volume flow rate of fuel was multiplied with density of the fuel.

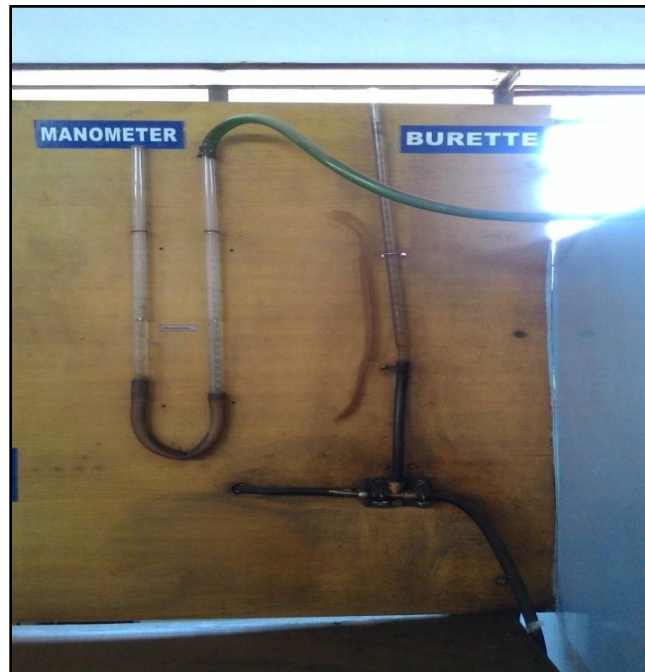


Figure 3.10: Fuel Burette

### 3.9 Temperature measurement

Various K type thermocouples are placed at different places to measure the temperature of exhaust gases, HRU inlet and outlet, energy storage materials at different places inside the shell. The K type thermocouple is inexpensive, and a wide variety of probes are available in its  $-200$  °C to  $+1350$  °C range.

## CFD MODELING AND SIMULATION

---

---

In the recent years the development of the Computational Fluid Dynamics (CFD) tool has made it possible to get a better understanding, analysis and solution of fluid flow and heat transfer problem in many applications. Analysis and simulation of various thermal systems can also be performed quite accurately with the help of CFD. Further, increasing computational power has enabled the researchers to create three-dimensional models using a fine grid for obtaining more accurate results.

CFD computer programs can be used to predict the fluid flow behavior. The majority of the CFD programs are based on the solution of the continuity equation, Navier- Stokes equations and the energy equation. CFD tools give a detailed knowledge of the pattern of fluid flow and the distribution of fluid velocity and temperature within an enclosed space, so the applications of CFD tools have become popular due to their deep-informative results with relatively less efforts and equipment costs involvement. CFD analysis is generally performed by using the commercial software FLUENT, PHOENIX, CFX etc., which work on finite volume method (FVM) based code for fluid flow simulations.

### 4.1 Overview of CFD simulation

CFD codes are mainly structured around the numerical algorithms that can solve fluid flow problems. To provide easy access to their solving power all commercial CFD packages consist of complex user interfaces to input problem parameters and to examine the results. Hence the codes contain three main elements: (i) a pre-processor (ii) a solver and (iii) a post-processor. The function of these elements within the context of a CFD code is explained in the following paragraphs.

#### 4.1.1 Pre- processor

Pre-processing means the input of a flow problem to a CFD program by means of an operator-friendly interface and the subsequent conversion of this input into a form which is suitable for use by the solver. The various user activities at the pre-processing stage includes the following:

- Definition of the geometry of the specified region of interest i.e. the computational domain.
- Grid generation i.e. dividing of the specified domain into a number of smaller, non-overlapping sub-domains: a grid or mesh of cells that act as control volumes or elements.
- Selection of the physical and chemical phenomena that need to be modeled.
- Definition of thermo-physical properties of fluids involved.
- Providing specifications of appropriate boundary conditions at cells which coincide with or touch the boundaries of domain being analyzed.

The accuracy of solution in CFD depends on the number, shape and size of cells in the grid. Apparently, larger the number of cells better is the accuracy of the solution. Both the accuracy of a solution and its cost in terms of necessary computer hardware and calculation time are dependent largely on the fineness of the grid. A CAD system is required for geometric modeling and grid generation.

#### 4.1.2 Solver

In this stage, numerical algorithms are used for solving the different equation of fluid flow and heat transfer. Finite volume method is most commonly used in CFD analysis. The numerical algorithm has the following important steps:

- First step is formal integration of different governing equations (continuity, momentum, energy etc.) of the fluid flow over the control volume of the solution domain.
- Second step is **discretization** which involves the substitution of a variety of finite difference type approximations for the terms in the integrated equation which represents flow processes such as convection, diffusion and sources. This integral equations are now converted into a system of algebraic equations.
- Third step is solving of the algebraic equations by an iterative method.

#### 4.1.3 Post-processor

Over past few years, a huge amount of development work has taken place in the field of post processing of CFD analysis. Due to the increasing popularity of engineering workstations over the years, many of which have outstanding graphics capabilities, the leading packages of CFD are now equipped with versatile data visualization tools. These include:

- Domain geometry and grid display.
- Vector plots.
- 2D and 3D surface plots.
- Particle tracking.
- View manipulation (translation, rotation, scaling etc.)
- Color postscript output.
- Animation for dynamic result display.

All commercially available codes produce trusty alphanumeric output and have data export facilities for further manipulation external to the code.

## **4.2 Problem solving steps in ANSYS-FLUENT**

Having determined the important feature of the problem to be solved, then the following basic procedural steps should be followed.

- i. Create the model geometry and mesh.
- ii. Start FLUENT by selecting the appropriate solver for 3D modeling
- iii. Select the solver formulation.
- iv. Choose the basic equations to be solved: laminaor or turbulent, radiation models, heat transfer models etc.
- v. Specify material properties.
- vi. Specify boundary conditions.
- vii. Adjust the solution parameters, initialize the flow field and calculate a solution by iteration.
- viii. Examine and write results.
- ix. Validate CFD results with experimental or any other results such as mathematical modeling results or results published by other researchers.

## **4.3 CFD model development**

The steps involved in the development of model of the Heat Recovery Unit and then its simulation process are as follows:

### 4.3.1 Geometrical modeling

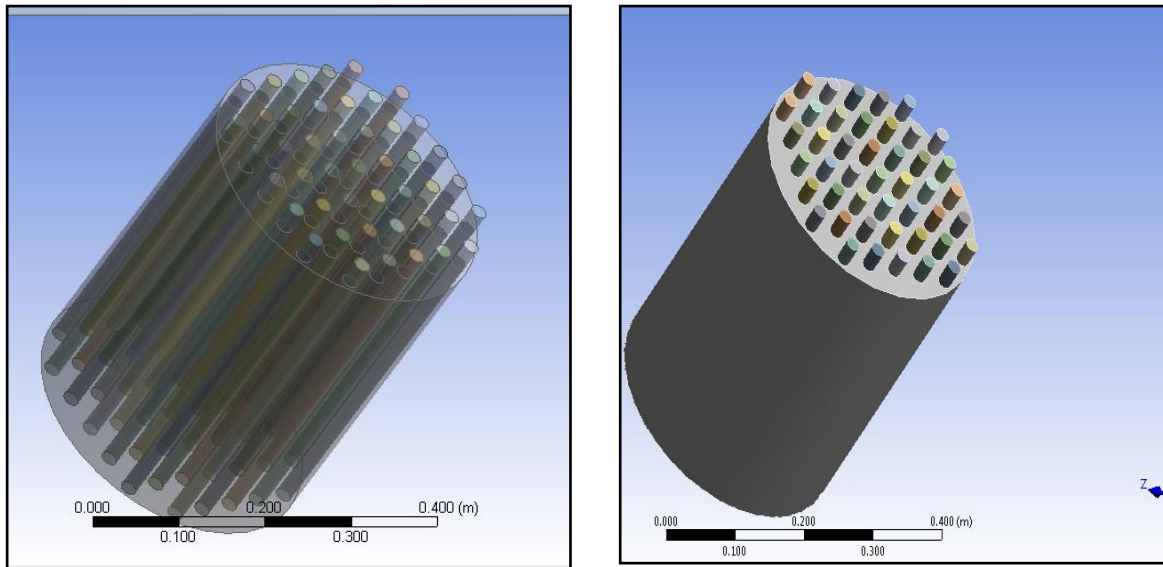


**Figure 4.1: Geometrical model of the Heat Recovery Unit**

The first step of any CFD analysis is the geometric modelling, wherein a real physical model is recreated in software with the exact specifications. In this work, the Heat Recovery Unit is modelled using SOLIDWORKS and then it is imported in ANSYS's DESIGN MODELER. In the actual model 4 fins are attached to each tubes of the Heat Recovery Unit, but for simplicity in simulation process the fins are not considered in the geometrical model.

Following pictures show arrangement of tubes in top and isometric views respectively.

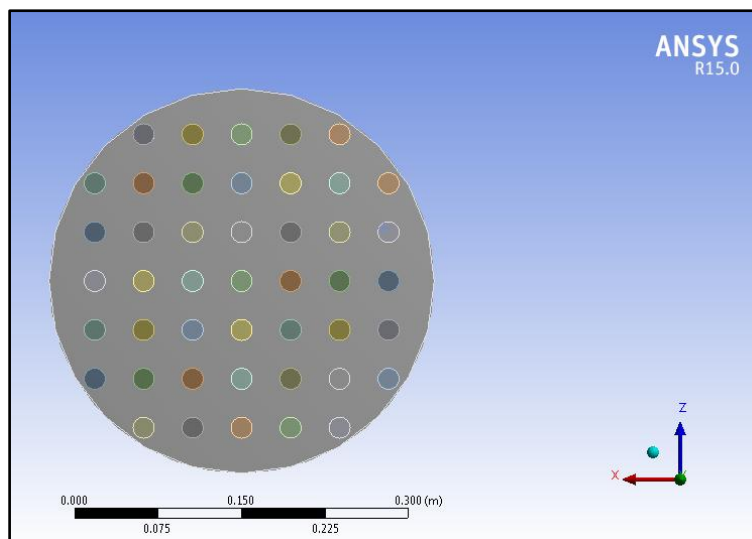


**Figure 4.2: Top view of the Heat Recovery Unit**

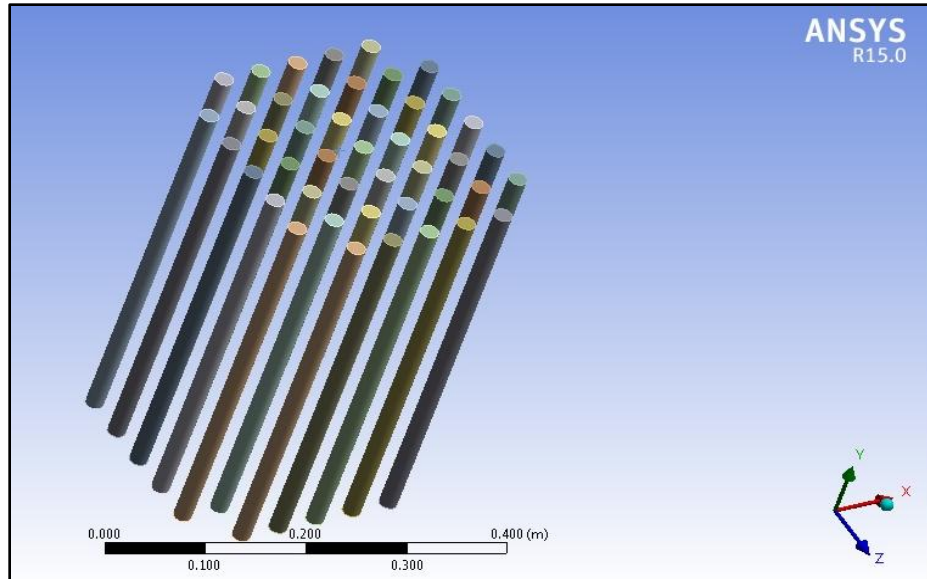


Figure 4.3: Isometric view of arrangement of the tubes

### 4.3.2 Mesh generation

Once the geometrical model is developed, the next step is to discretize its domain which is otherwise known as meshing. Meshing is the process of dividing the domain into large number of smaller units called cells. This is done to extract information about the parameters at each cell and node. Hexahedral element types were used to mesh the domain as shown below.

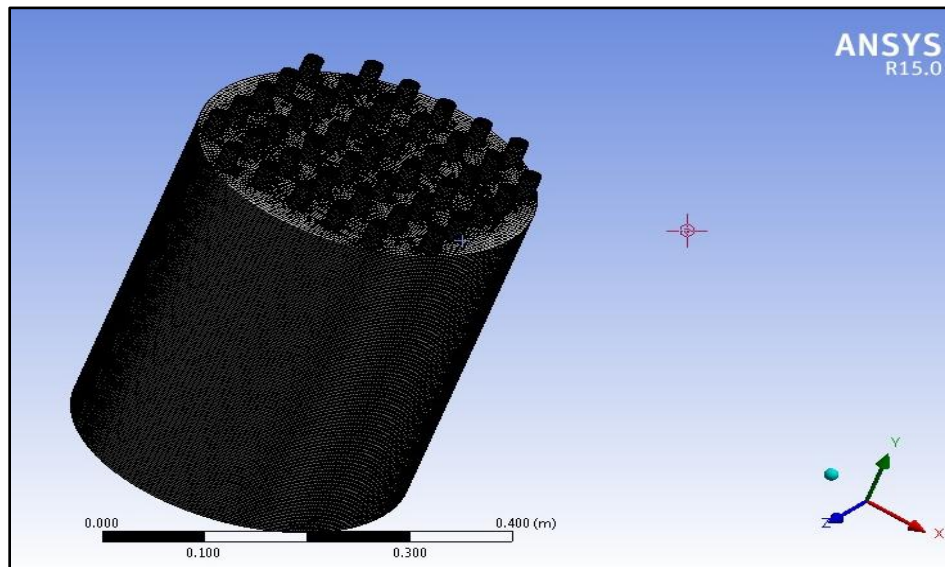
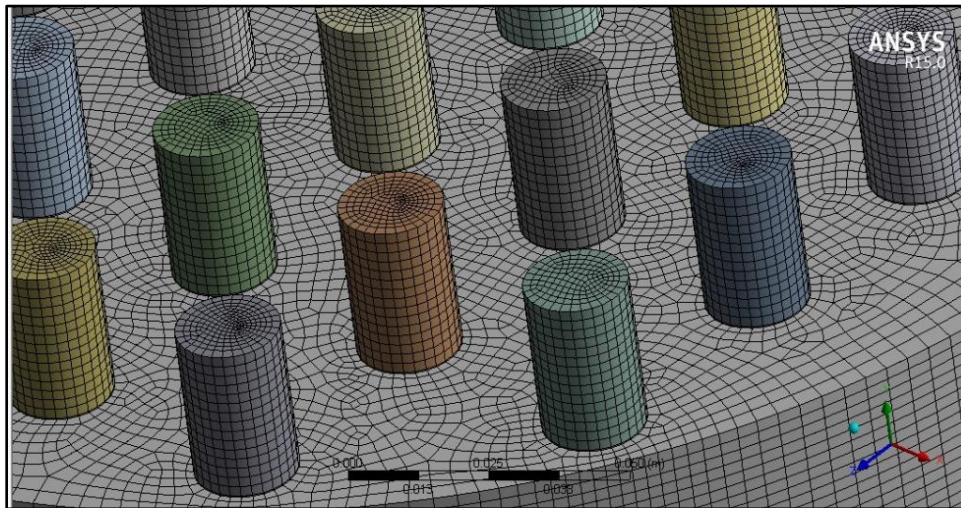


Figure 4.4: Meshing of the Heat Recovery Unit

It can be seen from Figure 4.4 that meshing of the tubes and shell are so fine that it is impossible to view the cells at this resolution. The statistics of the mesh are given below:

- Number of Nodes = 4338124
- Number of Elements = 4022261

The meshing of the tubes and shell can be clearly seen from the following pictures.



**Figure 4.5: Close up of shell and tubes mesh**

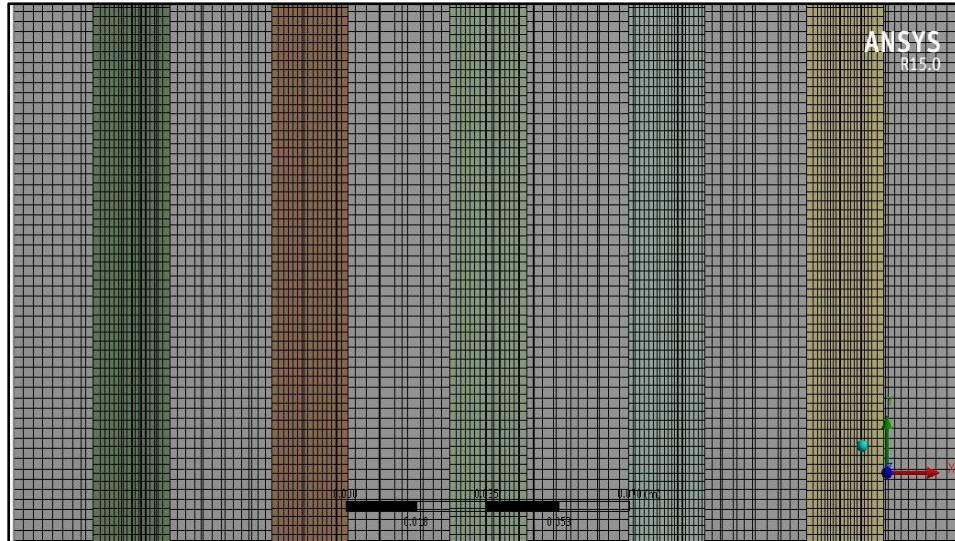


**Figure 4.6: Close up of mesh at the longitudinal mid-section of HRU**

There are a number of parameters like skewness, aspect ratio, orthogonal quality, element quality, warping factor etc. from which the quality of mesh could be checked, but the most important among these are skewness and aspect ratio.



**Skewness:** It determines how close the faces or cells are to ideal. The range and cell quality of skewness are given in the table below.

**Table 4.1: Scale of measuring mesh quality**

| Skewness | Cell Quality |
|----------|--------------|
| 1        | Degenerate   |
| 0.9-<1   | Bad (silver) |
| 0.75-0.9 | Poor         |
| 0.5-0.75 | Fair         |
| 0.25-0.5 | Good         |
| >0-0.25  | Excellent    |
| 0        | Equilateral  |

The obtained skewness values after meshing the model are as follows

**Table 4.2: Skewness of mesh**

| Skewness                  | Obtained Value |
|---------------------------|----------------|
| <b>Min.</b>               | 0.006833       |
| <b>Max.</b>               | 0.736557       |
| <b>Average</b>            | 0.171174       |
| <b>Standard Deviation</b> | 0.098508       |

Lesser the values of skewness, better is meshing. Overall skewness value of the model could better be represented by the average value obtained. Since 0.171174 is the average skewness value, we can infer that most of the faces or cells are meshed with *excellent quality*.

**Aspect Ratio:** It is the ratio of the longest edge length to the shortest edge length of a face or cell. A face or an element is considered perfect if its aspect ratio is 1. Aspect ratio's value more than 5 signifies bad quality.

The obtained values of aspect ratios are

**Table 4.3: Aspect ratios of mesh**

| Aspect Ratio       | Obtained Value |
|--------------------|----------------|
| Min.               | 1.0163         |
| Max.               | 10.405         |
| Average            | 1.766          |
| Standard deviation | 0.689          |

Since the average value of aspect ratio is 1.766, we can infer that the model has been meshed with *good quality*.

### 4.3.3 Named selection

In order to simplify the process of obtaining information about the required parameters at various locations on the Heat Recovery Unit, several faces have been given suitable names. After the simulation is run, as part of the post processing various parameters like pressure, temperature, velocities etc. on required faces or location could easily be obtained by calling these named selections. The named selections used for our simulation process are:

- Tube ( 1 to 45)
- Shell.
- Hot Fluid Inlet
- Hot Fluid Outlet.

#### 4.3.4 Assumptions taken in CFD simulation

- Fins which are attached to each tube in the experimental model of the Heat Recovery Unit are not considered in the geometrical model to avoid complexity in the simulation process.
- Heat transfer coefficient of the fluid around the tubes is assumed to be as high as  $300 \text{ W/m}^2\cdot\text{K}$  to compensate the absence of fins.
- It is assumed that the mass flow of exhaust air through each tube is the same. Also, the properties of the exhaust air are considered same as that of the ambient air.
- There is no source or sink of heat inside the fluid domain.
- Ambient air temperature is assumed to be 300 K.
- Heat loss from the Heat Recovery Unit to the environment is assumed to be negligible.

#### 4.4 CFD simulation

The Heat Recovery Unit Model after meshing is imported into Fluent and subjected to following set up solver:

**4.4.1 Mesh quality check:** Meshing is found to be of good quality.

**4.4.2 Solver:**

**Table 4.4: Solver set-up**

|                      |                |
|----------------------|----------------|
| Type                 | Pressure based |
| Velocity Formulation | Absolute       |
| Time                 | Steady         |

**4.4.3 Models**

- Energy
- Viscous model: k-epsilon (2 equation), Standard.
- Solidification and Melting (For CASE II simulation only)

#### 4.4.4 Materials:

##### Case I :

**Table 4.5: Material used for Case I**

|       |   |
|-------|---|
| Fluid | Tubes interior: Air<br>Shell interior: Shell Heat Transfer Oil S2 |
| Solid | Shell: Steel<br>Tubes: Steel                                      |

##### Case II:

**Table 4.6: Material used for Case II**

|       |   |
|-------|---|
| Fluid | Tubes interior: Air<br>Shell interior: PCM material ( Erythritol) |
| Solid | Shell: Steel<br>Tubes: Steel                                      |

#### 4.4.5 Boundary conditions

##### Case I:

**Table 4.7: Boundary conditions for Case I**

| Named Selection                   | Boundary Type   | Details   |
|-----------------------------------|-----------------|---|
| Tube ( 1 to 45)                   | Wall            | Material: Steel<br>Thickness= 0.001 m or 1 mm<br>Heat Transfer Coefficient= 300 W/m <sup>2</sup> .K |
| Shell                             | Wall            | Material: Steel<br>Thickness= 0.001 m or 1mm  |
| Hot Fluid Inlet<br>(Tube 1 to 45) | Velocity inlet  | Velocity= 0.47 m/s<br>Temperature =350 °C (For Charging condition)                                  |
| Hot Fluid Outlet                  | Pressure Outlet | Gauge Pressure = 0  |

**Case II**

**Table 4.8: Boundary conditions for Case II**

| <b>Named Selection</b>            | <b>Boundary Type</b> | <b>Details</b>  |
|-----------------------------------|----------------------|---|
| Tube ( 1 to 45)                   | Wall                 | Material: Steel<br>Thickness= 0.001 m or 1 mm<br>Heat Transfer Coefficient= 300 W/m <sup>2</sup> .K |
| Shell                             | Wall                 | Material: Steel<br>Thickness= 0.001 m or 1mm  |
| Hot Fluid Inlet<br>(Tube 1 to 45) | Velocity inlet       | Velocity= 0.47 m/s<br>Temperature =320 °C (For Charging condition)                                  |
| Hot Fluid Outlet                  | Pressure Outlet      | Gauge Pressure = 0  |

**4.4.6 Solution methods**

**Table 4.9: Solution methods used**

|                            |   |
|----------------------------|---|
| Pressure-Velocity Coupling | Scheme-Simple   |
| Spatial Discretization     | Gradient- Least Squares Cell Based<br>Pressure- Second Order<br>Momentum- Second Order Upwind<br>Turbulent Kinetic Energy- First Order Upwind<br>Turbulent Dissipation Rate- First Order Upwind |

#### 4.4.7 Solution controls

**Table 4.10: Under relaxation factors**

|                          |     |
|--------------------------|-----|
| Pressure                 | 0.3 |
| Density                  | 1   |
| Body Forces              | 1   |
| Momentum                 | 0.7 |
| Turbulent Kinetic Energy | 0.8 |

#### 4.4.8 Solution initialization: Hybrid initialization

Now that we have given all the necessary input data, the next step is to run the simulation process. After the simulation process is over, we can easily analyze the results with the help of graphs and contours.

In this study, we are basically simulating the temperature distribution over the HRU domain. The results and discussions are provided in the next chapter thoroughly.

**RESULTS AND DISCUSSIONS**

---

---

**5.1 Introduction**

This study is divided into two sections namely Case I and Case II. In Case I, the experimental and simulation results obtained by using thermic oil **Shell Heat Transfer Oil S2** as energy storage medium in the HRU are discussed. Further, in Case II, the experimental and simulation results obtained by using phase change material **Erythritol** as energy storage medium in the HRU are discussed. This study also deals with the analysis of the results obtained after running the simulation on HRU model and to check whether the model is validated or not. The HRU model is considered to be validated if the results obtained in the simulation are in agreement with those obtained experimentally.

**5.2 CASE I: THERMIC OIL AS ENERGY STORAGE MEDIUM**

The experiment was carried out on Kirloskar TAF1 stationary diesel engine integrated with the Heat Recovery Unit with Shell Heat Transfer Oil S2 as energy storage material. The time-temperature relationship at a load of 4.4 kW during the charging and discharging conditions are discussed in this section. Further, comparison between the experimental and simulation results is also shown in this section.

**5.2.1 Experimental results during charging condition**

Table 5.1 shows the variation in temperature of Thermic Oil at various places in the HRU with respect to time at a load of 4.4 kW during charging of the HRU. The reading has been taken at an interval of every 10 minutes for a period of 180 minutes, until Thermic oil reached its maximum steady temperature. The maximum temperature of Thermic Oil obtained was 182°C.

In table 5.1 T1, T2... upto T16 represents the temperatures of various thermocouples at different positions inside the HRU. Thermocouples no. 2, 5, 7, 8, 15 were placed near the centre position of the HRU, thermocouple no. 3, 4, 6, 10, 14 were placed in the intermediate position of the HRU and thermocouple no. 1, 9, 11, 12, 13, 16 lies near the outer position of the HRU. The pictorial view of various positions of the thermocouples is shown in figure 3.7.

**Table 5.1: Variation of Thermic oil temperature with respect to time at a load of 4.4 kW during charging of HRU (14 November 2016)**

| <b>T</b><br><b>(°C)</b> | <b>10</b><br><b>min</b> | <b>20</b><br><b>min</b> | <b>30</b><br><b>min</b> | <b>40</b><br><b>min</b> | <b>50</b><br><b>min</b> | <b>60</b><br><b>min</b> | <b>70</b><br><b>min</b> | <b>80</b><br><b>min</b> | <b>90</b><br><b>min</b> | <b>100</b><br><b>min</b> | <b>110</b><br><b>min</b> | <b>120</b><br><b>min</b> | <b>130</b><br><b>min</b> | <b>140</b><br><b>min</b> | <b>150</b><br><b>min</b> | <b>160</b><br><b>min</b> | <b>170</b><br><b>min</b> | <b>180</b><br><b>min</b> |
|-------------------------|-------------------------|-------------------------|-------------------------|-------------------------|-------------------------|-------------------------|-------------------------|-------------------------|-------------------------|--------------------------|--------------------------|--------------------------|--------------------------|--------------------------|--------------------------|--------------------------|--------------------------|--------------------------|
| <b>T<sub>1</sub></b>    | 32                      | 46                      | 60                      | 77                      | 91                      | 104                     | 115                     | 126                     | 133                     | 138                      | 146                      | 152                      | 158                      | 162                      | 168                      | 175                      | 179                      | 181                      |
| <b>T<sub>2</sub></b>    | 32                      | 51                      | 65                      | 81                      | 95                      | 108                     | 118                     | 130                     | 137                     | 142                      | 150                      | 156                      | 161                      | 166                      | 171                      | 176                      | 181                      | 182                      |
| <b>T<sub>3</sub></b>    | 33                      | 49                      | 63                      | 79                      | 93                      | 106                     | 116                     | 128                     | 135                     | 140                      | 148                      | 154                      | 159                      | 164                      | 169                      | 174                      | 179                      | 182                      |
| <b>T<sub>4</sub></b>    | 33                      | 48                      | 62                      | 78                      | 92                      | 105                     | 116                     | 127                     | 134                     | 141                      | 149                      | 155                      | 157                      | 165                      | 170                      | 175                      | 178                      | 181                      |
| <b>T<sub>5</sub></b>    | 33                      | 50                      | 64                      | 82                      | 95                      | 109                     | 119                     | 129                     | 138                     | 143                      | 151                      | 156                      | 162                      | 167                      | 172                      | 177                      | 181                      | 181                      |
| <b>T<sub>6</sub></b>    | 33                      | 47                      | 63                      | 80                      | 94                      | 107                     | 117                     | 127                     | 136                     | 141                      | 149                      | 154                      | 159                      | 165                      | 170                      | 175                      | 180                      | 182                      |
| <b>T<sub>7</sub></b>    | 33                      | 50                      | 64                      | 81                      | 94                      | 108                     | 119                     | 131                     | 138                     | 142                      | 150                      | 157                      | 161                      | 166                      | 172                      | 178                      | 182                      | 182                      |
| <b>T<sub>8</sub></b>    | 32                      | 52                      | 66                      | 80                      | 96                      | 110                     | 118                     | 129                     | 137                     | 142                      | 150                      | 156                      | 162                      | 167                      | 173                      | 178                      | 181                      | 182                      |
| <b>T<sub>9</sub></b>    | 33                      | 45                      | 61                      | 77                      | 90                      | 103                     | 115                     | 125                     | 132                     | 139                      | 147                      | 153                      | 157                      | 163                      | 167                      | 174                      | 178                      | 181                      |
| <b>T<sub>10</sub></b>   | 33                      | 48                      | 63                      | 79                      | 93                      | 107                     | 116                     | 128                     | 135                     | 140                      | 148                      | 155                      | 160                      | 164                      | 169                      | 175                      | 179                      | 181                      |
| <b>T<sub>11</sub></b>   | 33                      | 46                      | 61                      | 76                      | 89                      | 102                     | 114                     | 126                     | 133                     | 139                      | 146                      | 153                      | 156                      | 162                      | 166                      | 175                      | 179                      | 182                      |
| <b>T<sub>12</sub></b>   | 33                      | 45                      | 60                      | 75                      | 91                      | 103                     | 113                     | 126                     | 133                     | 138                      | 147                      | 152                      | 158                      | 163                      | 167                      | 176                      | 179                      | 182                      |
| <b>T<sub>13</sub></b>   | 33                      | 45                      | 61                      | 77                      | 90                      | 102                     | 115                     | 125                     | 132                     | 139                      | 146                      | 153                      | 156                      | 163                      | 165                      | 174                      | 178                      | 181                      |
| <b>T<sub>14</sub></b>   | 33                      | 47                      | 63                      | 79                      | 92                      | 107                     | 117                     | 127                     | 136                     | 141                      | 149                      | 155                      | 160                      | 165                      | 169                      | 175                      | 180                      | 182                      |
| <b>T<sub>15</sub></b>   | 33                      | 51                      | 65                      | 82                      | 94                      | 109                     | 120                     | 131                     | 139                     | 144                      | 152                      | 158                      | 163                      | 168                      | 174                      | 179                      | 182                      | 182                      |
| <b>T<sub>16</sub></b>   | 33                      | 46                      | 60                      | 76                      | 91                      | 102                     | 113                     | 125                     | 133                     | 139                      | 147                      | 153                      | 158                      | 163                      | 166                      | 175                      | 179                      | 182                      |

The graphical representation of the temperature of thermic oil at various locations inside the HRU with respect to time is shown in figure 5.1.



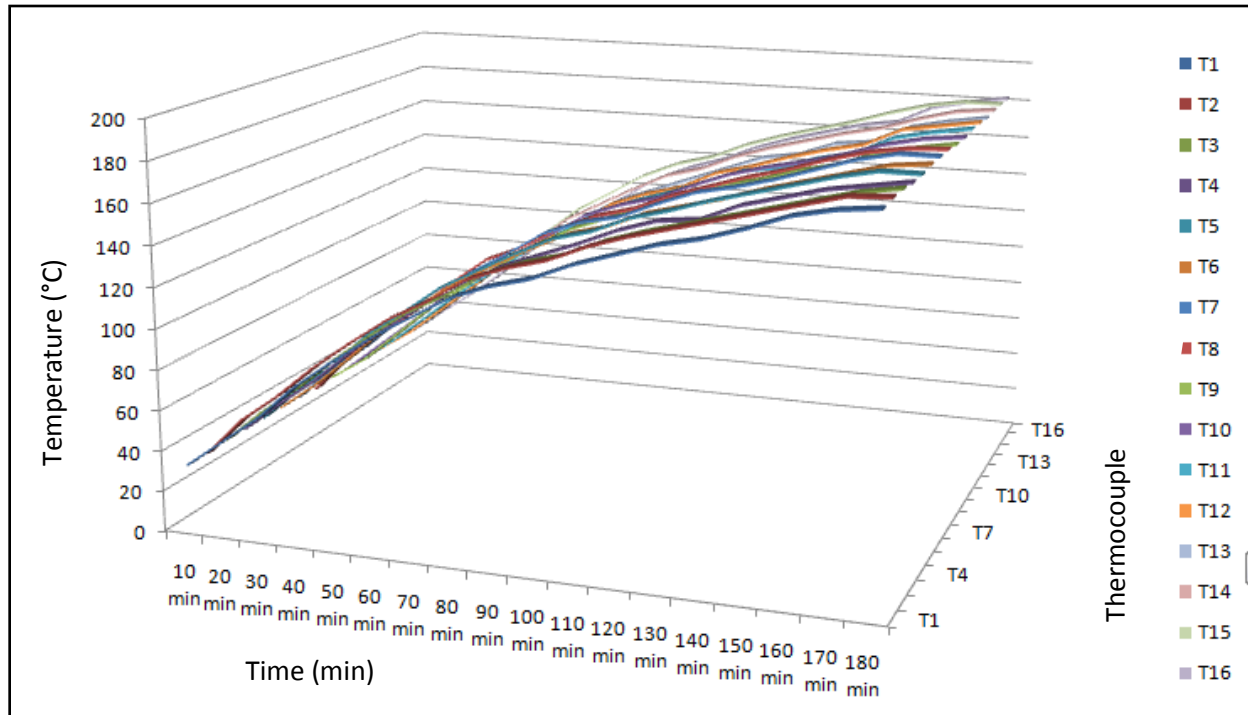


**Figure 5.1: Variation of Thermic oil temperature with respect to time at a load of 4.4 kW during charging of HRU (14 November 2016)**

It has been observed from figure 5.1 that there was approximately constant rise in temperature in the HRU. It can be also seen that rise in temperature of thermic oil at the centre position is higher as compared to outer (peripheral) position. This is due to the fact that exhaust gas is passing through a diverging section hence most of the effect of exhaust is at the centre. From the above figure it can be also seen that the maximum steady temperature attained by the thermic oil after a period of 180 minutes is 182 °C.

Figure 5.2 shows the variation of temperature of exhaust gas from the engine exhaust outlet, at the HRU inlet and at the HRU outlet with respect to time. It can be seen that the temperature of the exhaust gas from the engine exhaust outlet and at the HRU inlet had increased for some time and then it reached a steady value. Whereas, the temperature at the HRU outlet increased continuously until it reached the maximum steady temperature which is 182 °C. The maximum temperature of the exhaust gas recorded at the engine exhaust outlet and HRU inlet are 550 °C and 350 °C respectively. Further, it can be also seen that temperature of the exhaust gas at the engine exhaust pipe is not equal to the temperature at the HRU inlet. There is a drop in the temperature due to the heat loss from the pipe connecting the engine and the HRU.

In the figure 5.2,  $T_e$  represents the temperature at the exhaust outlet of the engine,  $T_i$  represents the temperature at the HRU inlet and  $T_o$  represents the temperature at the HRU outlet.

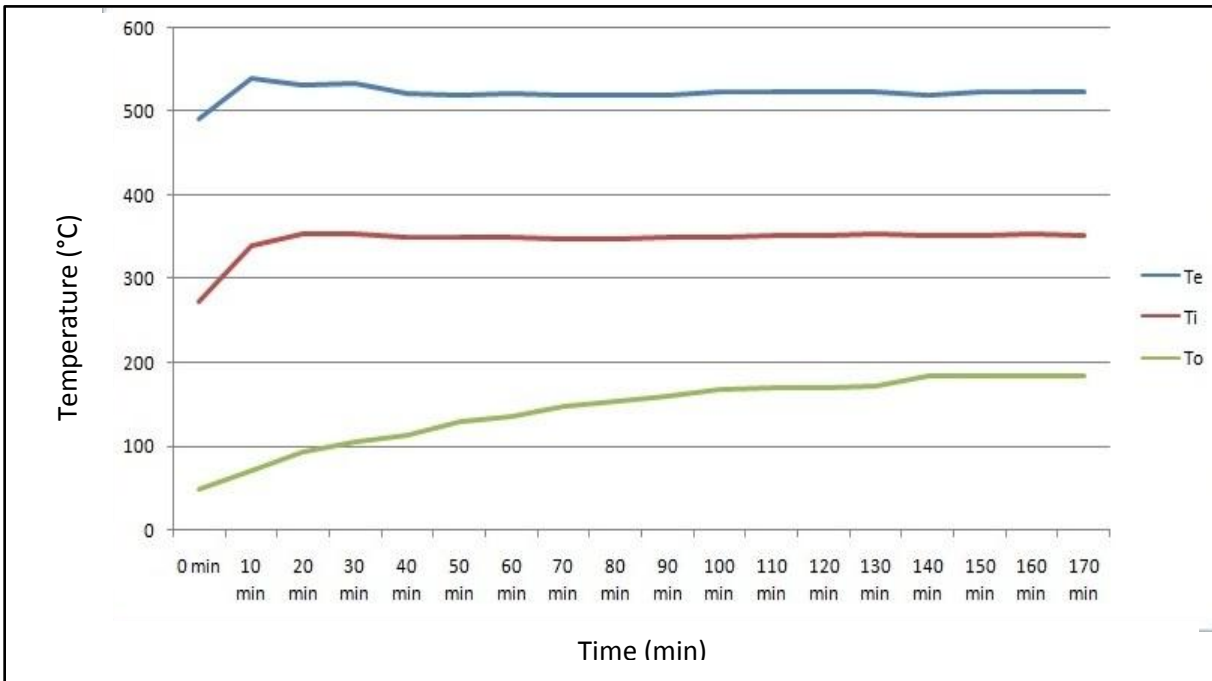


**Figure 5.2: Variation of  $T_e$ ,  $T_i$  and  $T_o$  with respect to time at load 4.4kW during charging of thermic oil (14 November 2016)**

### 5.2.2 Experimental results during discharging condition

Table 5.2 shows the drop in temperature of thermic oil at various places in the HRU with respect to time. The graphical representation of this variation of temperature of thermic oil with respect to time at different places in the HRU is shown in figure 5.3. From figure 5.3, it can be clearly seen that there was approximately constant decrease in temperature of thermic oil in HRU. It can be also seen that the temperature drop during discharging at the centre position and outer position is more as compared to intermediate position. This may be due to the fact that heat loss to environment at outer position is more as compared to intermediate position. Again, air is passing through the diverging section hence most of the effect of air is at centre tubes due to which temperature drop at centre is more.

**Table 5.2: Variation of Thermic oil temperature with respect to time during discharging of HRU (14 November 2016)**

| <b>T (°C)</b>         | <b>0 min</b> | <b>10 min</b> | <b>20 min</b> | <b>30 min</b> | <b>40 min</b> | <b>50 min</b> | <b>60 min</b> | <b>70 min</b> | <b>80 min</b> | <b>90 min</b> |
|-----------------------|--------------|---------------|---------------|---------------|---------------|---------------|---------------|---------------|---------------|---------------|
| <b>T<sub>1</sub></b>  | 181          | 175           | 166           | 162           | 156           | 151           | 146           | 141           | 135           | 129           |
| <b>T<sub>2</sub></b>  | 182          | 174           | 167           | 163           | 158           | 153           | 148           | 143           | 137           | 130           |
| <b>T<sub>3</sub></b>  | 181          | 177           | 169           | 165           | 159           | 154           | 149           | 144           | 138           | 133           |
| <b>T<sub>4</sub></b>  | 181          | 178           | 171           | 167           | 161           | 157           | 153           | 147           | 140           | 134           |
| <b>T<sub>5</sub></b>  | 182          | 174           | 166           | 162           | 156           | 152           | 147           | 142           | 135           | 130           |
| <b>T<sub>6</sub></b>  | 181          | 177           | 168           | 164           | 159           | 155           | 149           | 144           | 136           | 132           |
| <b>T<sub>7</sub></b>  | 182          | 175           | 167           | 163           | 157           | 153           | 148           | 144           | 136           | 131           |
| <b>T<sub>8</sub></b>  | 181          | 175           | 166           | 161           | 156           | 152           | 147           | 144           | 135           | 130           |
| <b>T<sub>9</sub></b>  | 181          | 174           | 167           | 162           | 156           | 152           | 147           | 141           | 135           | 130           |
| <b>T<sub>10</sub></b> | 181          | 177           | 169           | 165           | 159           | 155           | 149           | 144           | 137           | 133           |
| <b>T<sub>11</sub></b> | 181          | 174           | 167           | 162           | 157           | 153           | 148           | 144           | 136           | 130           |
| <b>T<sub>12</sub></b> | 181          | 173           | 166           | 161           | 157           | 152           | 147           | 143           | 135           | 130           |
| <b>T<sub>13</sub></b> | 181          | 174           | 167           | 162           | 156           | 152           | 146           | 141           | 134           | 129           |
| <b>T<sub>14</sub></b> | 182          | 177           | 170           | 165           | 159           | 155           | 148           | 143           | 135           | 131           |
| <b>T<sub>15</sub></b> | 181          | 175           | 167           | 162           | 157           | 152           | 147           | 142           | 136           | 132           |
| <b>T<sub>16</sub></b> | 181          | 174           | 166           | 161           | 156           | 152           | 146           | 142           | 135           | 131           |

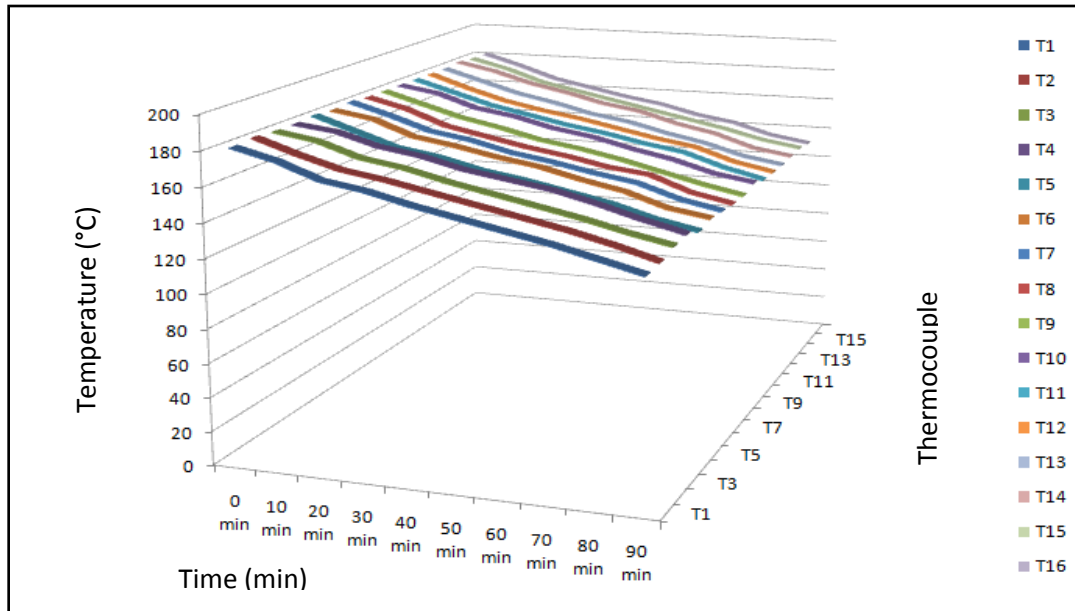


**Figure 5.3: Variation of Thermic oil temperature with respect to time during discharging of HRU (14 November 2016)**

Figure 5.4 shows the variation of temperature of air which is blown by the blower at the inlet and outlet of the HRU.  $T_i$  represents the temperature of air at the inlet of HRU while  $T_o$  represents the temperature of air at the outlet of HRU. From the figure it can be seen that the temperature of air at the HRU inlet is constant which is at room temperature. But the temperature of air at the HRU outlet decreases with time due to the decrease in temperature of thermic oil inside the HRU during discharging.

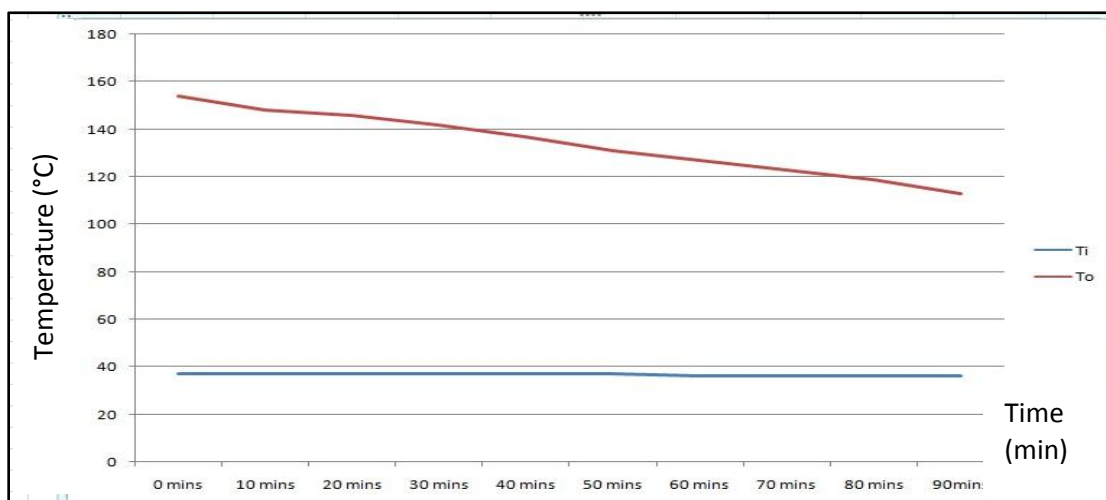


**Figure 5.4: Variation of  $T_i$  and  $T_o$  with time during discharging of HRU (14 November 2016)**

### 5.2.3 Results on simulation of HRU model

The geometrical model of the Heat Recovery Unit has been simulated. The simulation results have been shown in the form of temperature contours.

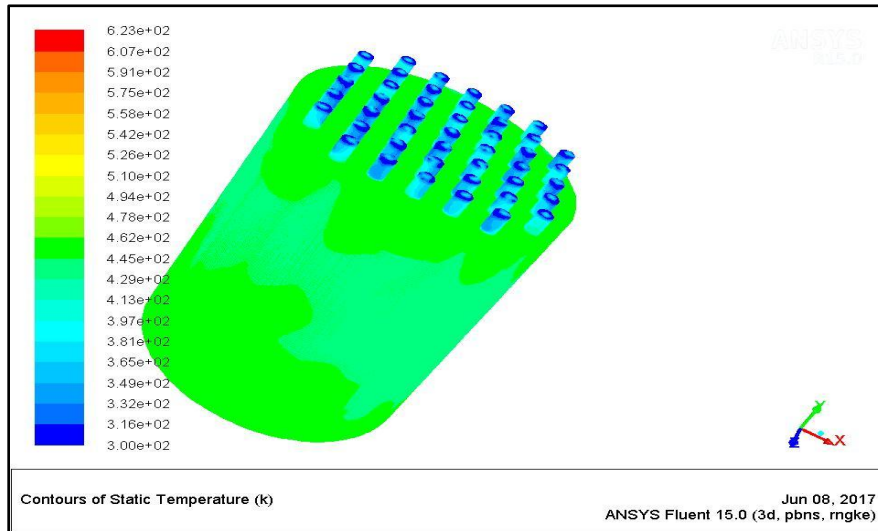
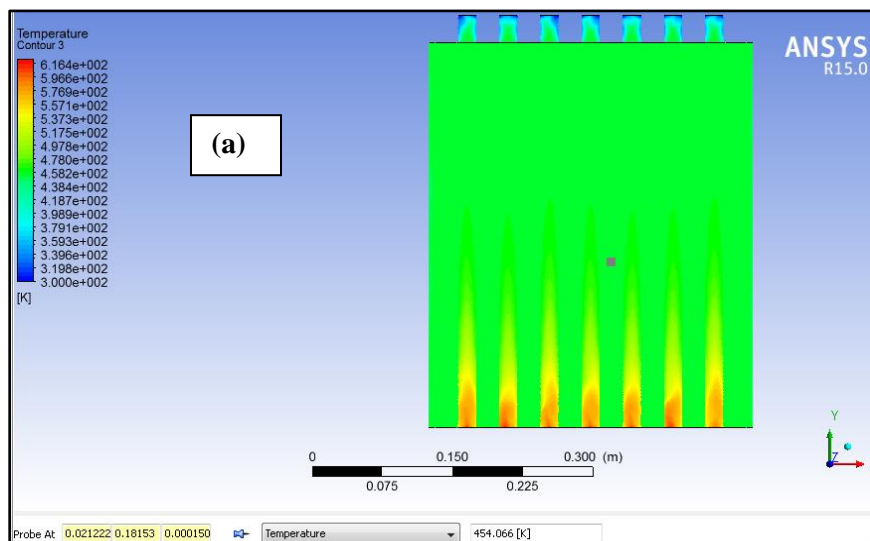
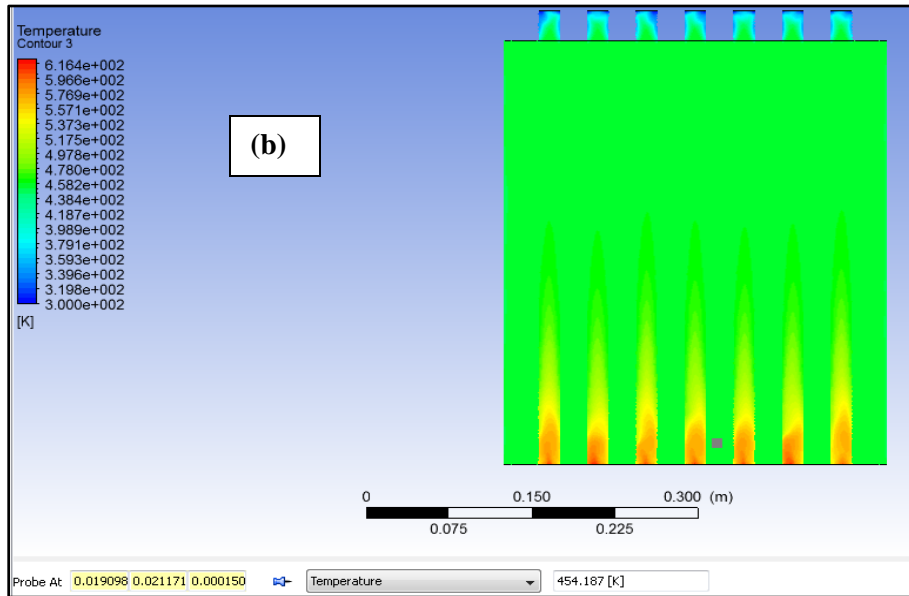


**Figure 5.5: Temperature contour of the HRU model (using Thermic Oil as ESM) during charging**  
 In order to check the temperature of thermic fluid and temperature of exhaust gas at the HRU outlet, a longitudinal mid-section plane of the HRU has been considered and the temperature contours have been shown in that plane.

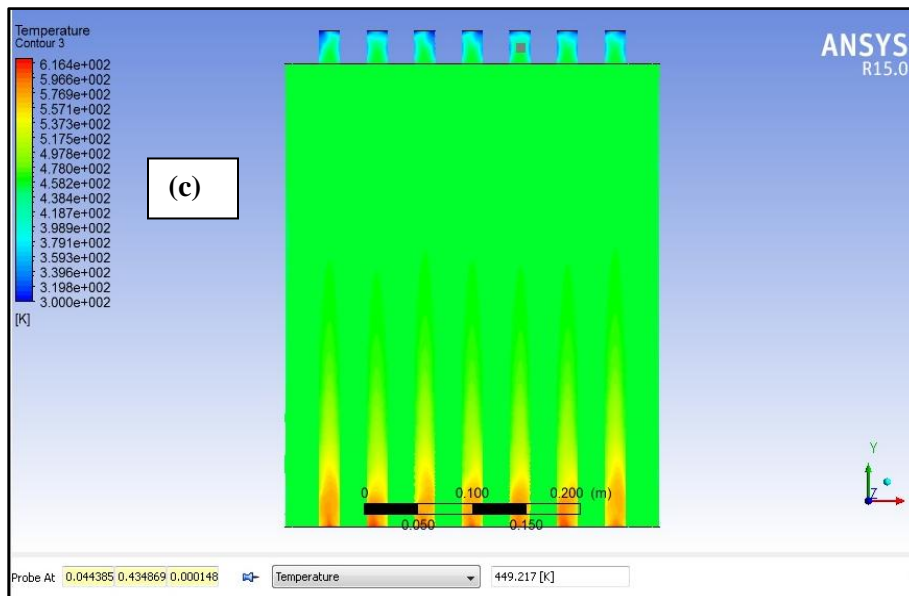
### CHARGING CONDITION



*(a) Probe showing temperature of thermic oil at the middle of HRU*



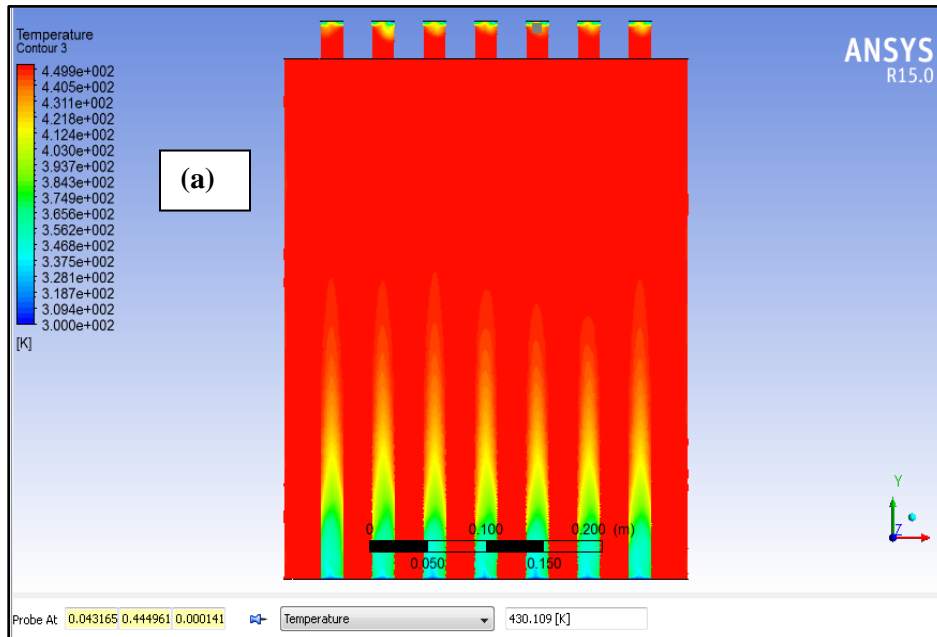
(b) Probe showing temperature of thermic oil at the bottom of HRU



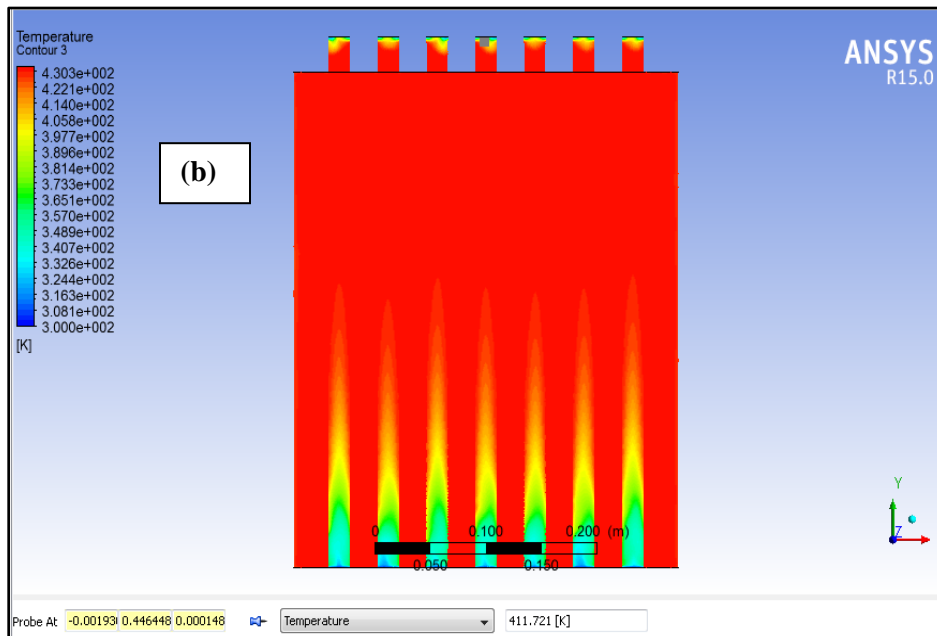
(c) Probe showing temperature of exhaust gas the HRU outlet

**Figure 5.6: Temperature contour at longitudinal mid-section plane of HRU during charging condition (using Thermic Oil as ESM)**

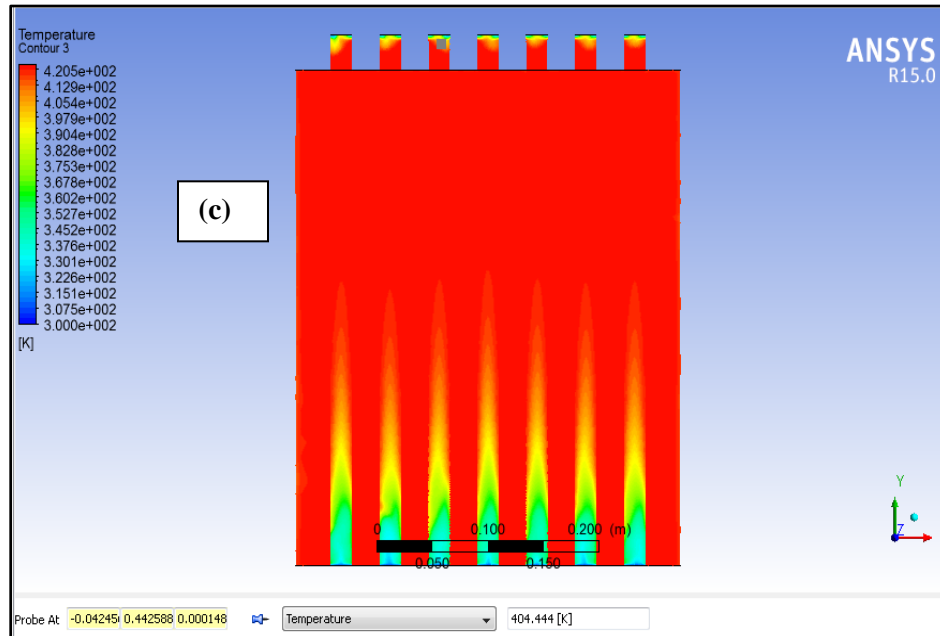
## **DISCHARGING CONDITION**



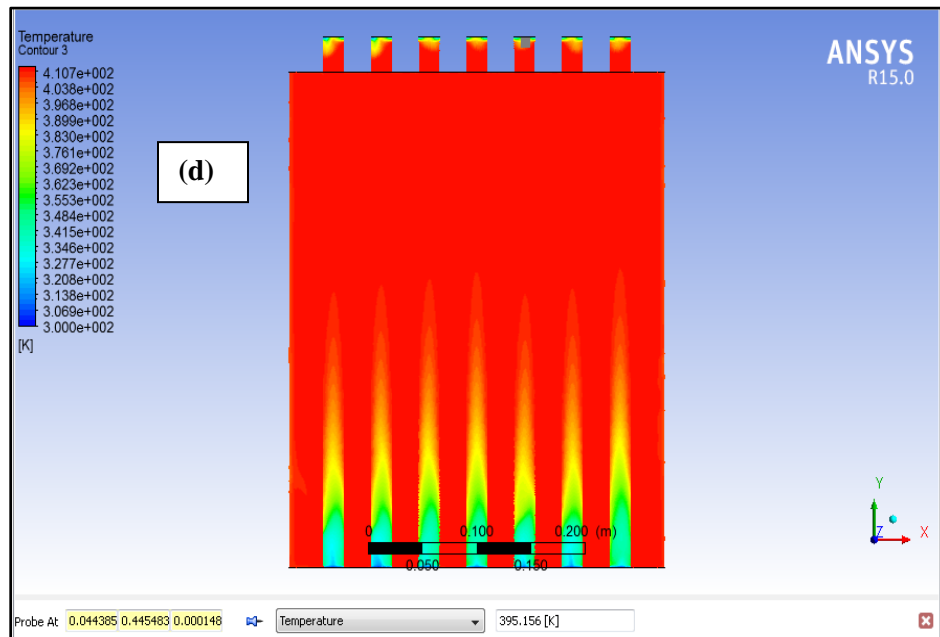
(a) Probe showing temperature of exhaust gas when the temperature of thermic oil is 175 °C



(b) Probe showing temperature of exhaust gas when the temperature of thermic oil is 155 °C

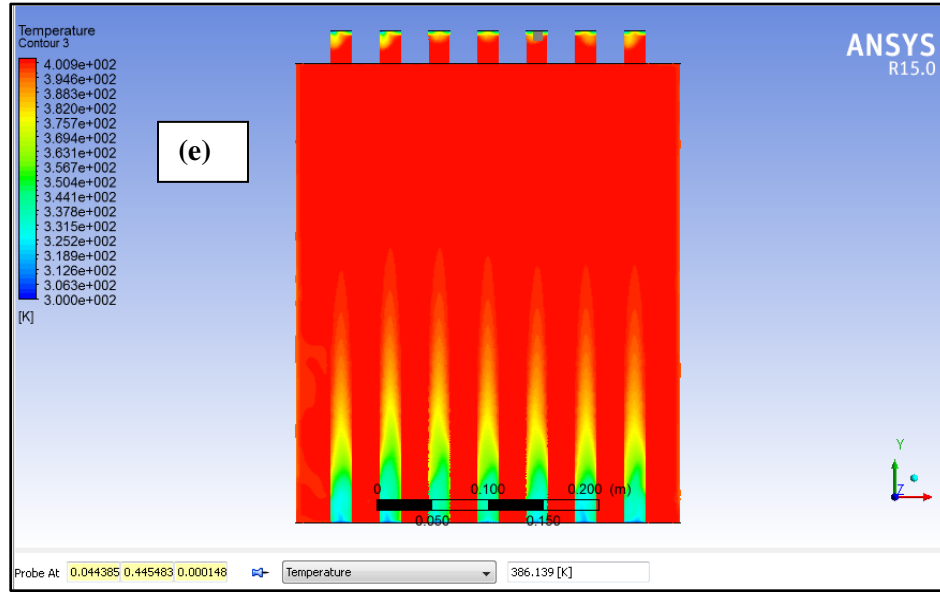


(c) Probe showing temperature of exhaust gas when the temperature of thermic oil is 145 °C



(d) Probe showing temperature of exhaust gas when the temperature of thermic oil is 135 °C





(e) Probe showing temperature of exhaust gas when the temperature of thermic oil is 125 °C

**Figure 5.7: Temperature contour at longitudinal mid-section plane of HRU during discharging condition (using Thermic Oil as ESM)**

### 5.2.4 Results on validation

The geometrical model of the HRU developed for validation as per the experimental set up has been simulated. The simulation has been carried out both for the charging and the discharging condition of the HRU.

Following is the comparison between experimental and simulation results obtained during **charging** of HRU.

**Table 5.3: Comparison between experimental and simulation results during charging (using Thermic Oil as ESM)**

|   | Experimental(°C) | Simulation(°C) | Error( %) |
|---|------------------|----------------|-----------|
| <b>Maximum temperature of Thermic oil inside HRU</b>        | 182              | 181.187        | 0.44      |
| <b>Maximum temperature of exhaust gas at the HRU outlet</b> | 182              | 176.217        | 3.17      |

Following is the comparison between experimental and simulation results obtained during **discharging** of HRU.

**Table 5.4: Comparison between experimental and simulation results during discharging (using Thermic Oil as ESM)**

| Thermic oil temperature (°C) | Temperature of HRU outlet (experimental) (°C) | Temperature of HRU outlet (simulation) (°C) | Error (%) |
|------------------------------|---|---|-----------|
| 175                          | 158   | 157.109                                     | 0.56      |
| 155                          | 139   | 138.721                                     | 0.20      |
| 145                          | 132   | 131.444                                     | 0.42      |
| 135                          | 123   | 122.156                                     | 0.69      |
| 125                          | 115   | 113.139                                     | 1.61      |

The following graph shows the comparison between experimental and simulation results during discharging condition

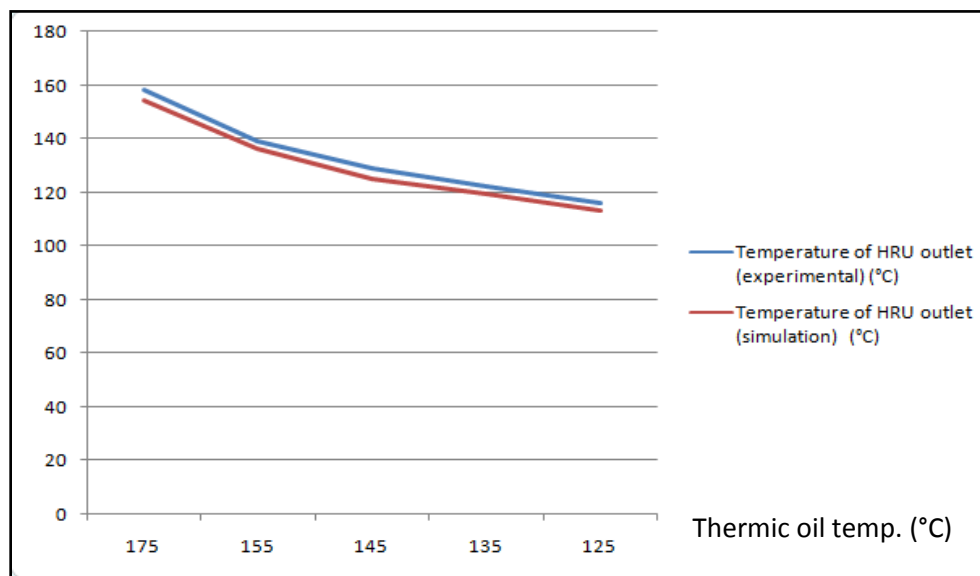


**Figure 5.8: Comparison between experimental and simulation results during discharging (using Thermic Oil as ESM)**

Variation between experimental and simulation results

- Minimum error = 0.44 %
- Maximum error = 3.17 %
- Average error = 1.01 %

It is clear that the results obtained from simulation are in reasonably proximity with those from the experiment. So, it is safe to infer that the model of the HRU stands validated and that the simulated results obtained are credible.

### **5.3 CASE II: ERYTHRITOL AS ENERGY STORAGE MEDIUM**

The experiment was carried out on Kirloskar TAF1 stationary diesel engine integrated with the Heat Recovery Unit with Erythritol as energy storage material. The time-temperature relationship at a load of 1.8 kW during charging and discharging conditions are discussed in this section. Further, comparison between the experimental and simulation results is also shown in this section. The experimental results of PhD Research Scholar Mr. Dheeraj Kishor Johar have been used to validate the HRU model.

#### **5.3.1 Experimental results during charging condition**

Figure 5.9 shows the rise in temperature of Erythritol (phase change material, to reach the melting point temperature from atmospheric temperature, approx. 30<sup>0</sup>C) at various places in HRU with respect to time at a load of 1.8 kW during charging condition. At a load of 4.4 kW temperatures reached above the melting point temperature (after complete melting) in 65 minutes. The maximum steady temperature reached after 65 minutes is 126 °C.

21 thermocouples were placed at different places in the HRU. Thermocouple No. 1, 4, 7, 10, 13, 16 and 19 were placed at a height of 100 mm from the bottom. Thermocouple No. 2, 5, 8, 11, 14, 17, 20 were placed at a height of 200 mm from bottom and Thermocouple No. 3, 6, 9, 12, 15, 18 and 21 were placed at a height of 300 mm from the bottom. It has been observed from figure 5.9 that there is approximately constant rise in temperature in HRU. Further, it has been observed that the rise in temperature of erythritol at centre position is higher as compared to outer

(peripheral) position. This is due to the fact that exhaust is passing through a diverging section and hence most of the effect of exhaust is at the centre tubes.

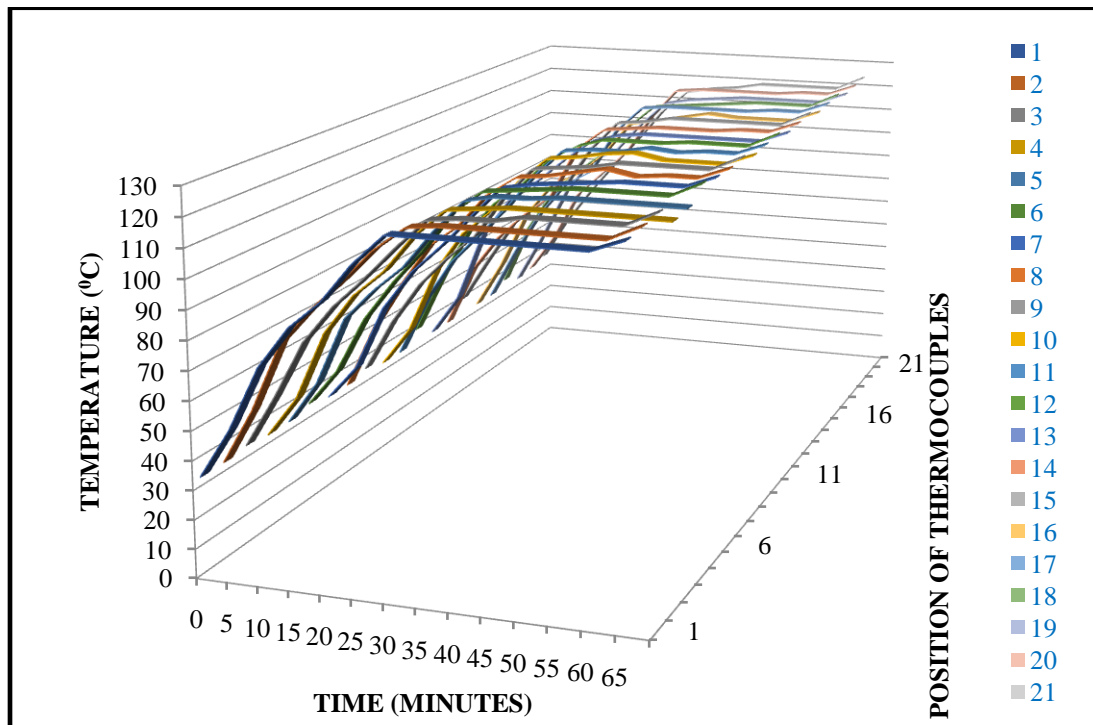


**Figure 5.9: Variation of temperature of Erythritol with respect to time at a load of 4.4 kW during charging of HRU**

### 5.3.2 Experimental results during discharging condition

Figure 5.10 shows the drop in temperature of Erythritol at various places in the HRU with respect to time. It has been observed from figure 5.10 that there was approximately constant decrease in temperature in HRU. Also it has been seen that temperature drop during discharging at centre position and outer position is more as compared to intermediate position. This may be due to the fact that heat loss to environment at outer position is more compared to intermediate position. Again air is passing through the diverging section hence most of the effect of air is at centre tubes due to which temperature drop at the centre is more. During discharging temperature of Erythritol inside the HRU dropped from 126 °C to 90 °C during a time interval of 105 minutes.

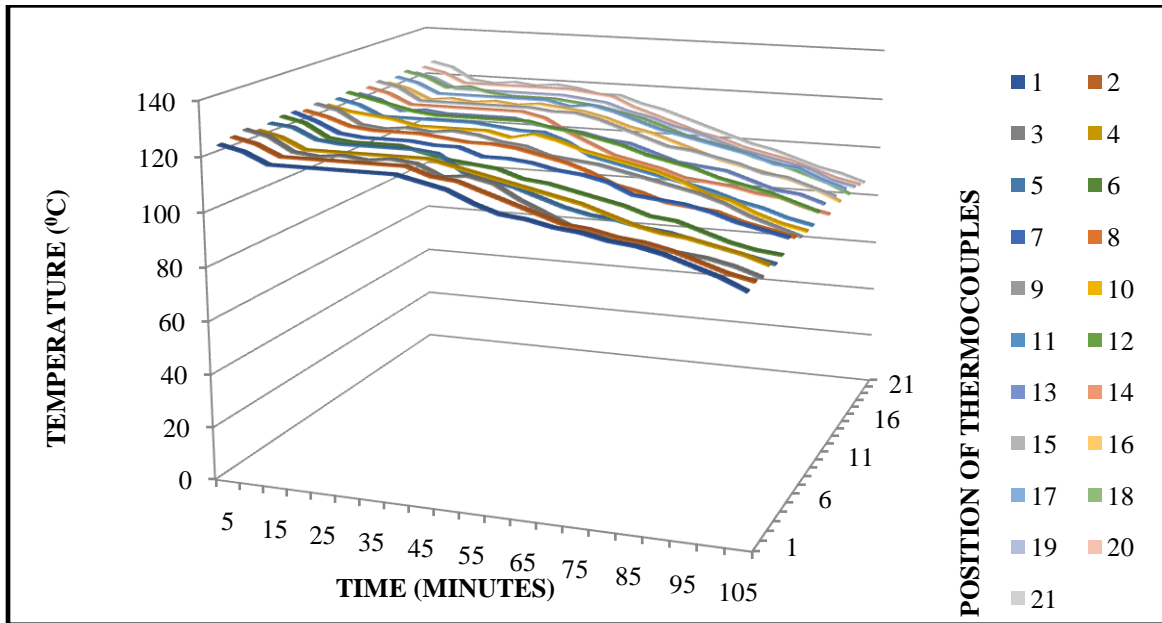


Figure 5.10: Variation of temperature of Erythritol with respect to time during discharging of HRU

### 5.3.3 Results on simulation of HRU model

The geometrical model of the Heat Recovery Unit has been simulated. The simulation results have been shown in the form of temperature contours.

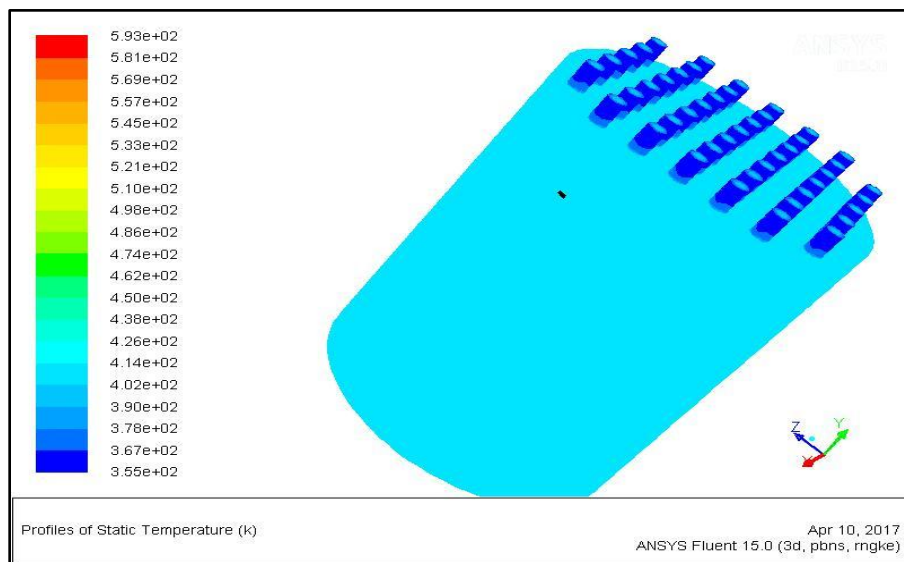
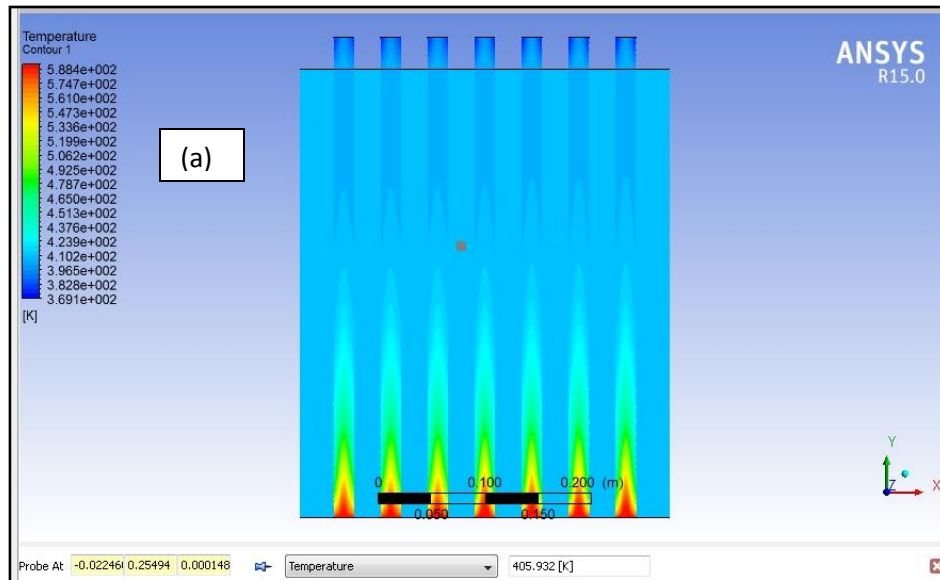


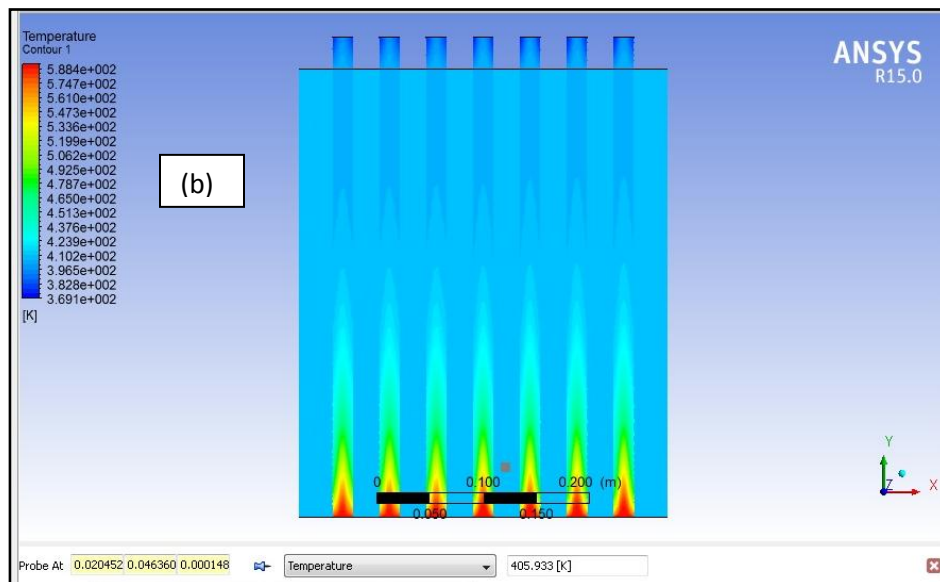
Figure 5.11: Temperature contour of the HRU model (using Erythritol as ESM) during charging

In order to check the temperature of Erythritol and temperature of exhaust gas at the HRU outlet, a longitudinal mid-section plane of the HRU has been considered and the temperature contours have been shown in that plane.

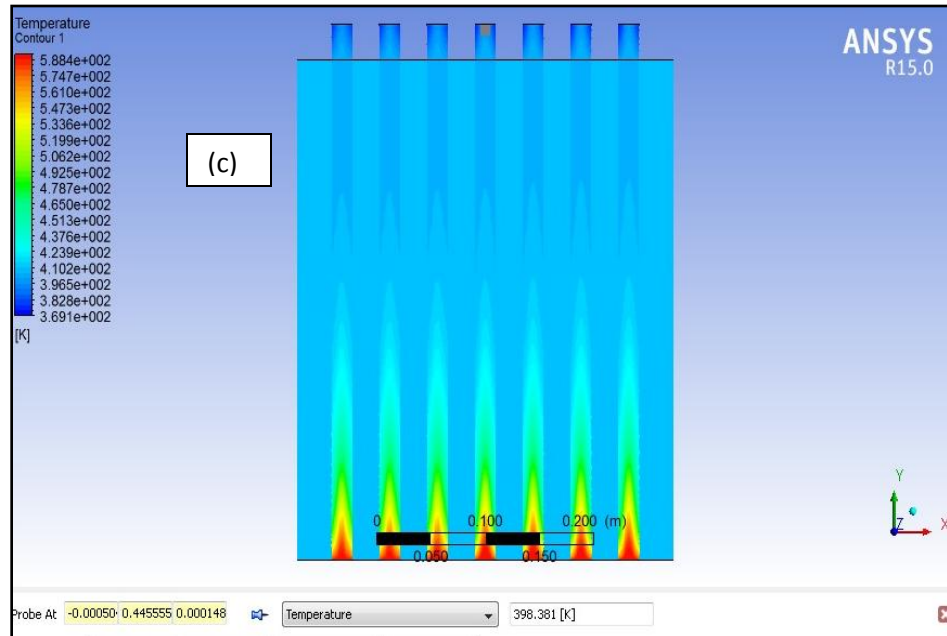
### **CHARGING CONDITION**



(a) Probe showing temperature of Erythritol at the middle of HRU



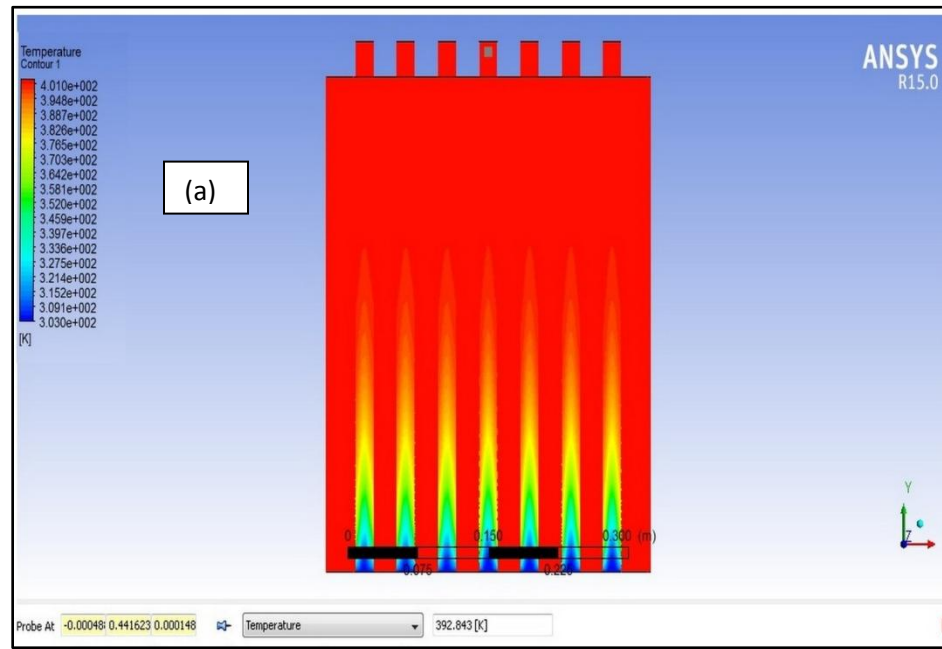
(b) Probe showing temperature of Erythritol at the bottom of HRU



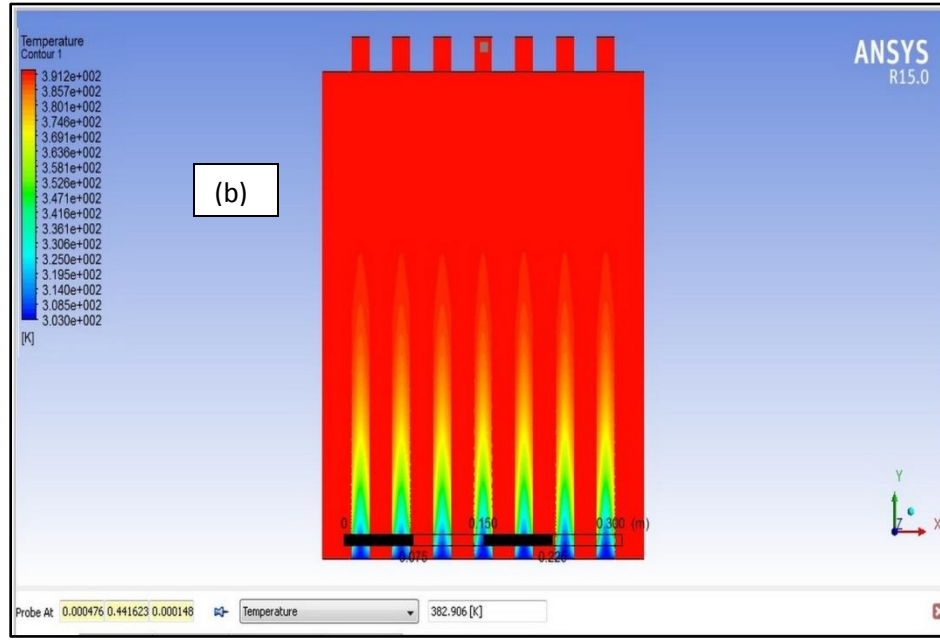
(c) Probe showing temperature of exhaust gas the HRU outlet

**Figure 5.12: Temperature contour at longitudinal mid-section plane of HRU during charging condition (with Erythritol as ESM)**

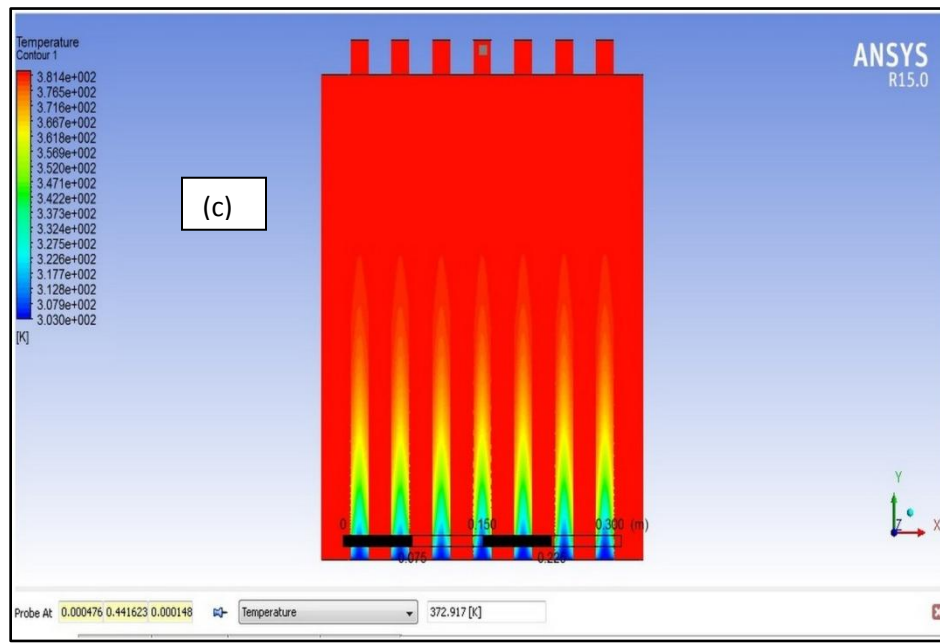
### DISCHARGING CONDITION



(a) Probe showing temperature of exhaust gas when the temperature of Erythritol is 126 °C

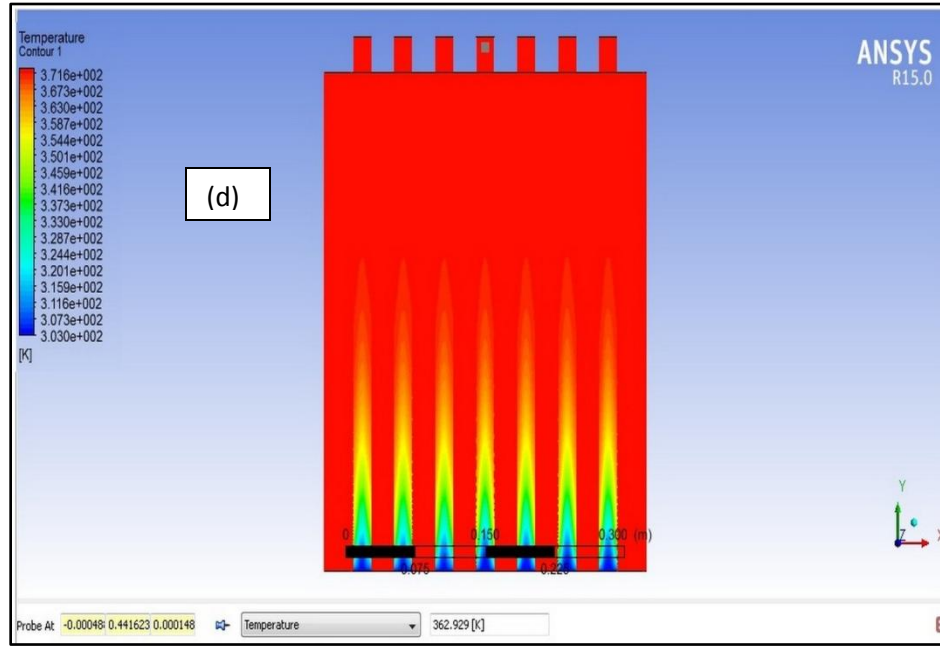


(b) Probe showing temperature of exhaust gas when the temperature of Erythritol is 120 °C



(c) Probe showing temperature of exhaust gas when the temperature of Erythritol is 110 °C





(d) Probe showing temperature of exhaust gas when the temperature of Erythritol is 100 °C

**Figure 5.13: Temperature contour at longitudinal mid-section plane of HRU during discharging condition (with Erythritol as ESM)**

### 5.3.4 Results on validation

The geometrical model of the HRU developed for validation as per the experimental set up has been simulated. The simulation has been carried out both for the charging and the discharging condition of the HRU.

Following is the comparison between experimental and simulation results obtained during **charging** of HRU

**Table 5.5: Comparison between experimental and simulation results during charging (with Erythritol as ESM)**

|   | Experimental(°C) | Simulation(°C) | Error( %) |
|---|------------------|----------------|-----------|
| <b>Maximum temperature of Erythritol inside HRU</b>         | 126              | 132.933        | 5.50      |
| <b>Maximum temperature of exhaust gas at the HRU outlet</b> | 126              | 125.381        | 0.49      |

Following is the comparison between experimental and simulation results obtained during **discharging** of HRU.

**Table 5.6: Comparison between experimental and simulation results during discharging (with Erythritol as ESM)**

| Thermic oil temperature (°C) | Temperature of HRU outlet (experimental) (°C) | Temperature of HRU outlet (simulation) (°C) | Error (%) |
|------------------------------|---|---|-----------|
| 125                          | 117   | 119.843                                     | 2.42      |
| 120                          | 108   | 109.906                                     | 1.91      |
| 110                          | 97  | 99.917                                      | 3.01      |
| 100                          | 87  | 89.929                                      | 3.36      |

The following graph shows the comparison between experimental and simulation results during discharging condition

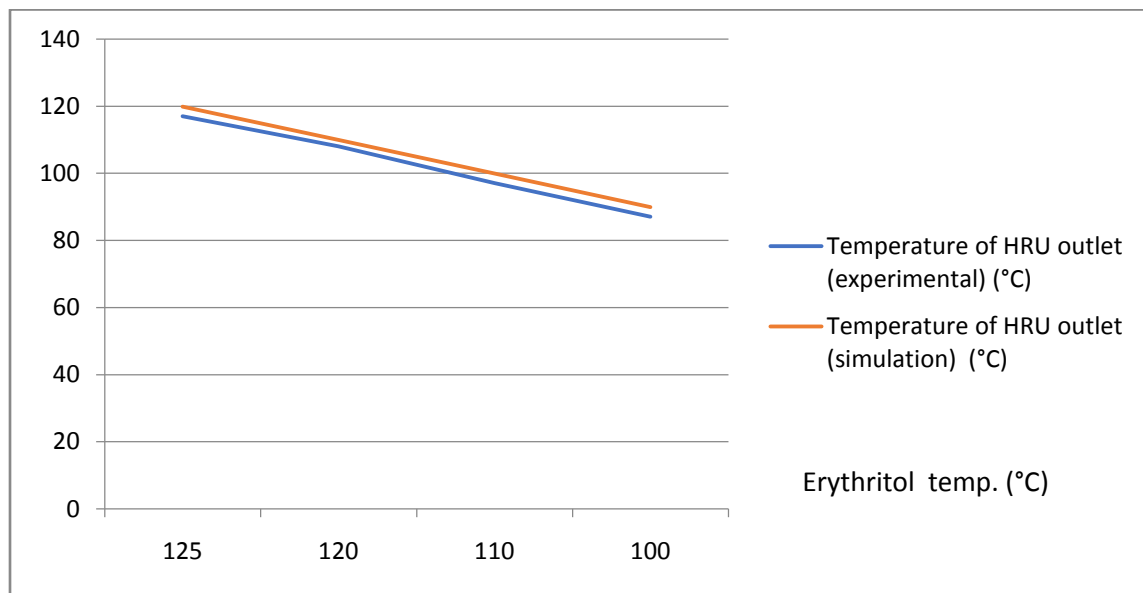


**Figure 5.14: Comparison between experimental and simulation results during discharging (with Erythritol as ESM)**

Variation between experimental and simulation results

- Minimum error = 0.49 %
- Maximum error = 5.50 %
- Average error = 2.78 %

It is clear that the results obtained from simulation are in reasonably proximity with those from the experiment. So, it is safe to infer that the model of the HRU stands validated and that the simulated results obtained are credible.

## 6.1 Conclusion

It is imperative to draw following useful conclusions from the exhaustive study conducted through the course of one year, involving experimental analysis and CFD simulation of a Heat Recovery Unit (HRU) which is recovering waste heat from the exhaust of a stationary C.I. engine:

- The experimental analysis was carried out with a stationary C.I engine integrated with the Heat Recovery Unit (HRU).
- From the experimental study it has been identified that there is a large potential of energy saving through the use of Heat Exchangers (HRU) as waste energy recovery technique.
- Maximum temperature achieved by Thermia S2 during charging condition of HRU was 182 °C after a period of 180 minutes when operated under full load (4.4 kW).
- Maximum temperature achieved by Erythritol during charging condition of HRU was 126 °C after a period of 65 minutes when operated under full load (4.4 kW).
- Successfully modeled, simulated and validated the HRU model using Fluent programme in the ANSYS Workbench 15.0
- The simulation of the HRU was carried out for two different heat storage materials: Shell Heat Transfer Oil S2 (Thermic Oil) and Erythritol (Phase Change Material). For each material, the simulation was carried for both the charging and the discharging conditions.
- The average error (between the simulation and experimental results) obtained while using thermic oil and PCM as thermal energy storage materials in the HRU are 1.01% and 2.78% respectively. Since the model is validated, the simulation results obtained are credible.
- Developed model was able to predict the temperature distribution inside the HRU with reasonable accuracy.

## 6.2 Future Scope

Following recommendations are proposed for future work:

- In this work the fins attached to the tubes of the HRU are not considered for CFD analysis. So CFD analysis of the HRU considering the effect of the fins could be carried out.
- Although in this study the CFD analysis has been carried out for steady state condition, but for better analysis, simulation could be done considering transient condition
- CFD simulation may be carried out to optimize the heat transfer performance of the HRU so that it can be used in a much effective manner.
- The heat storage capacity of the HRU can be predicated by carrying out CFD simulation considering different thermal storage materials.

## REFERENCES

1. Kim Tae Young, Negash Assmelash A., Cho Gyubaek, *Waste heat recovery of a diesel engine using a thermoelectric generator equipped with customized thermoelectric modules*, Energy Conversion and Management 124, 2016, 280-286.
2. Kim Young Min, Shin Dong Gil, Kim Chang Gi, Cho Gyu Baek, *Single-loop organic Rankine cycles for engine waste heat recovery using both low-and-high –temperature heat sources*, Energy 96, 2016, 482-494.
3. Johar Dheeraj Kishor, Sharma Dilip, Soni Shyam Lal, Gupta Pradeep K., Goyal Rahul, *Experimental investigation on latent heat thermal energy storage system for C.I. engine exhaust exhaust*, Applied Thermal Engineering 104, 2016, 64-73.
4. Wang Jialong, Wu Jingyin, Wang Hongbin, *Experimental investigation of a dual-source powered absorption chiller based on gas engine waste heat and solar thermal energy*, Energy, 2015. 1-10.
5. Goyal Rahul, Sharma Dilip, Soni S.L., Gupta Pradeep Kumar, Johar Dheeraj, *An experimental investigation of CI engine operated micro-cogeneration system for power and space cooling*, Energy Conversion and Management 89, 2015, 63-70.
6. Wang Jialong, Wu Jingyi, *Investigation of a mixed effect absorption chiller powered by jacket water and exhaust gas waste heat of internal combustion engine*, International Journal of Refrigeration 50, 2015, 193-206.
7. Fu Jianqin, Liu Jingping, Xu Zhengxin, Ren Chengqin, Deng Banglin, *A combined thermodynamic cycle based on methanol dissociation for IC (internal combustion) engine exhaust heat recovery*, Energy 55, 2013, 778-786.
8. Fu Jianqin, Liu Jingping, Xu Zhengxin, Ren Chengqin, Deng Banglin, Wang Linjun, *An open steam power cycle used for IC engine exhaust gas energy recovery*, Energy 44, 544-554.
9. Keinath Christopher M, Delahanty Jared C, Garimella Srinivas, Garrabrant Michael A, *Diesel engine waste-heat driven ammonia-water absorption system for space conditioning applications*, International Refrigeration and Air Conditioning Conference, July 16-19, 2012.

10. Pandiyaeajan V., Chinnappandian M., Raghavan V., Velraj R. “*Second law analysis of a diesel engine waste heat recovery with a combined sensible and latent heat storage system*, Energy Policy 39, 2011, 6011-6020.
11. AlQdah Khaled S, *Performance and evaluation of aqua ammonia auto air conditioner system using exhaust waste energy*, Energy Procedia 6, 2011, 467-476.
12. Manzela Andre Aleixo, Hanriot Sergio Morais, Gomez Luben Cabezas, Sodre Jose Ricardo, *Using engine exhaust gas as energy source for an absorption refrigeration system*, Applied Energy 87, 2010, 1141-1148.
13. Khatri Kamal Kishore, Sharma Dilip, Soni S.L., Tanwar Deepak, *Experimental investigation of CI engine operated Micro-Trigeneration system*, Applied Thermal Engineering 30, 2010, 1505-1509.
14. Jiangzhou S, Wang R.Z., Lu Y.Z, Xu Y.X, Wu J.Y, *Experimental study on locomotive driver cabin adsorption air conditioning prototype machine*, Energy Conversion and Management 46, 2005, 1655-1665.
15. Temizer Ilker, Ilkilic Cumali, *The performance and analysis of the thermoelectric generator system used in diesel engines*, Renewable and Sustainable Energy Reviews 63, 2016, 141-151.
16. Bhore Ketan, Bhosale Sharad, *Waste heat recovery of IC engine using VAR system*, International Engineering Research Journal, June 2016, 223-229, ISSN 2395-1621.
17. Wang Enhua, Zhang Hongguang, Fan Boyuan, Ouyang Minggao, Kai Yang, Yang Fuyuan, Li Xiaojuan, Wang Zhen, *3D numerical analysis of exhaust flow inside a fin and tube evaporator used in engine waste heat recovery*, Energy, 2015, 1-13.
18. Dong Chenxuan, Lu Yiji, wang Liwei, Roskilly Anthony Paul, *Design and assessment on a novel integrated system for power and refrigeration using waste heat from diesel engine*, Applied Thermal Engineering 91, 2005, 591-599.
19. Sowjanya S. Lakshmi, *Thermal analysis of a car air conditioning system based on an absorption refrigeration cycle using energy from exhaust gas of an internal combustion engine*, Advanced engineering and Applied Science: An International Journal 3, 2013, 47-53.

20. Saidur R, Rezaei M, Muzammil W.K, Hassan M.H, Paria S, Hasanuzzaman, *Technologies to recover exhaust heat from internal combustion engines*, Renewable and Sustainable Energy Reviews 16, 2012, 5649-5659.
21. Wang Tianyou, Zhang Yajun, Peng Zhijun, Shu Gequn, *A review of researches on thermal exhaust heat recovery with Rankine cycle*, Renewable and Sustainable Energy Reviews 15, 2011, 2862-2871.
22. Li S., Wu J.Y., *Theoretical research of a silica gel-water adsorption chiller in a micro combined cooling, heating and power (CCHP) system*, Applied Energy 86, 2009, 958-967.
23. Talbi M, Agnew B, *Energy recovery from diesel engine exhaust gases for performance enhancement and air conditioning*, Applied Thermal Engineering 22, 2002, 693-702.
24. Meunier F., *Adsorptive Cooling: A clean technology*, Clean Production Process 3, 2001, 8-20.
25. Koehler J, Tegethoff WJ, Westphalen D, Sonnekalb M, *Absorption refrigeration system for mobile applications utilizing exhaust gases*, Heat and Mass Transfer 32, 1997, 333-340.
26. Jadho JS, Thombare DG, *Review on exhaust gas heat recovery for IC engine*, International Journal of Engineering and Innovative Technology 2, 2013, 93-100.
27. *Waste Heat Recovery: Technologies and Opportunities in US industries*, US Department of Energy, March 2008.



## APPENDIX-A

### Governing equations

The numerical model of the HRU is based on continuity equation, the momentum equation, the energy equation and the k-ε equation. The k-ε equation is one of the most common turbulence models, which is built in FLUENT and gives good results for bounded wall and internal flows with small mean pressure gradients

#### I. Conservation of mass equation or Continuity equation

Differential equation can be derived when control mass is considered. For infinity minimal mass the conservation of mass equation can be written in general form as follows:

$$\frac{\partial \rho}{\partial t} + \nabla \cdot (\rho V) = 0$$

#### II. Conservation of momentum equations

For the expression of the conservation of momentum Newton's second law is explained as follows: the net force that affects the control mass and the fluent piece mass of the control mass is the multiplication of the mass control fluent piece and the acceleration is equal to the net momentum speed derived from the control mass.

In the conservation of momentum equation, different diagrams can be written for various coordinates. In the most general form, the momentum equations for three different coordinate levels are as follow:

X-momentum :

$$\begin{aligned} \frac{\partial(\rho u)}{\partial t} + \frac{\partial(\rho uv)}{\partial y} + \frac{\partial(\rho u^2)}{\partial x} + \frac{\partial(\rho uw)}{\partial z} \\ = -\frac{\partial \rho}{\partial x} + \frac{\partial}{\partial x} \left( \lambda \nabla \cdot V + 2\mu \frac{\partial u}{\partial x} \right) + \frac{\partial}{\partial y} \left[ \mu \left( \frac{\partial v}{\partial x} + \frac{\partial u}{\partial y} \right) \right] + \frac{\partial}{\partial z} \left[ \mu \left( \frac{\partial u}{\partial z} + \frac{\partial w}{\partial x} \right) \right] + \rho f_x \end{aligned}$$

### Y-momentum

$$\begin{aligned} \frac{\partial(\rho v)}{\partial t} + \frac{\partial(\rho uv)}{\partial x} + \frac{\partial(\rho v^2)}{\partial y} + \frac{\partial(\rho vw)}{\partial z} \\ = -\frac{\partial \rho}{\partial y} + \frac{\partial}{\partial y} \left( \lambda \nabla \cdot V + 2\mu \frac{\partial v}{\partial y} \right) + \frac{\partial}{\partial x} \left[ \mu \left( \frac{\partial v}{\partial x} + \frac{\partial u}{\partial y} \right) \right] + \frac{\partial}{\partial z} \left[ \mu \left( \frac{\partial v}{\partial z} + \frac{\partial w}{\partial y} \right) \right] + \rho f_y \end{aligned}$$

### Z -momentum

$$\begin{aligned} \frac{\partial(\rho w)}{\partial t} + \frac{\partial(\rho vw)}{\partial y} + \frac{\partial(\rho uw)}{\partial x} + \frac{\partial(\rho w^2)}{\partial z} \\ = -\frac{\partial \rho}{\partial z} + \frac{\partial}{\partial z} \left( \lambda \nabla \cdot V + 2\mu \frac{\partial w}{\partial z} \right) + \frac{\partial}{\partial x} \left[ \mu \left( \frac{\partial w}{\partial x} + \frac{\partial u}{\partial z} \right) \right] + \frac{\partial}{\partial y} \left[ \mu \left( \frac{\partial v}{\partial z} + \frac{\partial w}{\partial y} \right) \right] + \rho f_z \end{aligned}$$

### III. Energy equation

The energy equation can be represented as:

$$\frac{\partial(\rho e)}{\partial t} + \nabla \cdot (\rho e V) = \frac{\partial}{\partial x} \left( k \frac{\partial T}{\partial x} \right) + \frac{\partial}{\partial y} \left( k \frac{\partial T}{\partial y} \right)$$

### IV. Turbulence equations

In this study k-ε turbulence model is selected. According to this model, turbulence distribution and kinetic energy equations are as follows

$$\rho \frac{Dk}{Dt} = \frac{\partial}{\partial x_i} \left[ \left( \mu + \frac{\mu t}{\sigma k} \right) \frac{\partial k}{\partial x_i} \right] + Gk + Gb - \rho \epsilon - Ym$$

$$\rho \frac{D\epsilon}{Dt} = \frac{\partial}{\partial x_i} \left[ \left( \mu + \frac{\mu t}{\sigma \epsilon} \right) \frac{\partial \epsilon}{\partial x_i} \right] + C1s \frac{\epsilon}{k} (Gk + G3sGb) - C2s\rho \frac{\epsilon^2}{k}$$

$$\mu t = \rho C_\mu \frac{k^2}{\epsilon}$$

In this equation, Gk represents generation of turbulence kinetic energy due to mean velocity gradients, Gb is the generation of turbulence kinetic energy due to buoyancy, Ym represents the fluctuating dilation in compressible turbulence to the overall dissipation rate.

**APPENDIX-B****Specifications of the TES materials used.****Table B.1: Technical specifications of Shell Heat Transfer Oil S2**

| <b>Properties</b>                | <b>Values</b>         |
|----------------------------------|-----------------------|
| Density (at 40°C)                | 850 kg/m <sup>3</sup> |
| Kinematic Viscosity (at 40°C)    | 25 mm <sup>2</sup> /s |
| Specific Heat Capacity (at 40°C) | 1.954 kJ/kg.K         |
| Thermal Conductivity (at 40°C)   | 0.133 W/mK            |
| Flash Point                      | 220 °C                |
| Fire Point                       | 255 °C                |
| Pour Point                       | -12 °C                |
| Initial Boiling Point            | 355 °C                |
| Autoignition Temperature         | 360 °C                |

**Table B.2: Technical Specifications of Erythritol**

| <b>Properties</b>              | <b>Values</b>                                 |
|--------------------------------|---|
| Density (at 30°C)              | 1450 kg/m <sup>3</sup>                        |
| Dynamic Viscosity (at 30°C)    | 0.799 m.Pa.s                                  |
| Specific Heat Capacity         | 2.61 kJ/kg.K (liquid)<br>2.25 kJ/kg.K (solid) |
| Thermal Conductivity (at 30°C) | 0.733 W/mK                                    |
| Latent Heat                    | 339.8 kJ/kg                                   |
| Melting Temperature            | 117.7°C                                       |

## APPENDIX-C

### Thermocouples and their applications

Table C.1: Different thermocouples and their applications

| Thermocouple type | Conductors  | Temperature range (°C) | Typical specified temperature range (°C) | Application environments      |
|-------------------|---|------------------------|--|-------------------------------|
| <b>E</b>          | Chromel (+)<br>Constantan (-)                           | -270 to +1000          | -200 to +900                             | Oxidizing. Inert,<br>vacuum   |
| <b>J</b>          | Iron(+)<br>Constantan (-)                               | -210 to +1200          | 0 to +760                                | Oxidizing, reducing,<br>inert |
| <b>T</b>          | Copper (+)<br>Constantan (-)                            | -270 to +400           | -200 to +371                             | Corrosive, moist,<br>subzero  |
| <b>K</b>          | Chromel (+)<br>Alumel (-)                               | -270 to +1370          | -200 to +1260                            | Inert                         |
| <b>N</b>          | Nicrosil (+)<br>Nisil (-)                               | -270 to +1300          | 0 to +1260                               | Oxidizing                     |
| <b>B</b>          | Platinum (30% Rhodium) (+)<br>Platinum (6% Rhodium) (-) | 0 to +1820             | 0 to +1820                               | Oxidizing, inert              |
| <b>S</b>          | Platinum (10% Rhodium) (+)<br>Platinum (-)              | -50 to +1760           | 0 to +1480                               | Oxidizing, inert              |
| <b>R</b>          | Platinum (13% Rhodium) (+)<br>Platinum (-)              | -50 to 1760            | 0 to +1480                               | Oxidizing, inert              |

## PUBLICATIONS

---

---

Das Swaraj, Inda Chandrapal Singh, Sharma Dilip, “*Waste Heat Recovery from the Exhaust of Internal Combustion Engines for the Purpose of Refrigeration and Air Conditioning: A Review*”, ISST Journal of Mechanical Engineering, Vol 7, No. 1 (January-July 2016), p.p15-21, (ISSN 0976-7371)

# WASTE HEAT RECOVERY FROM THE EXHAUST OF INTERNAL COMBUSTION ENGINES FOR THE PURPOSE OF REFRIGERATION AND AIR CONDITIONING: A REVIEW

<sup>1</sup> Swaraj Das, <sup>1</sup> Chandrapal Singh and <sup>2</sup> Dilip Sharma

<sup>1</sup> M.Tech. (Thermal Engineering), Malaviya National Institute of Technology, Jaipur-302017, Rajasthan, India

<sup>1</sup> Professor, Mechanical Engineering, Malaviya National Institute of Technology, Jaipur-302017, Rajasthan, India  
E-mail: swaraj.das30@gmail.com, sharmadmnit@gmail.com

MS Received Through: RESSD-2016, held on October 7-8, 2016, at JECRC, Jaipur

## ABSTRACT

The depletion of fossil fuels is a serious concern now a days. Internal combustion engines are one of the major consumers of fossil fuels. A large amount of energy from the internal combustion engine is wasted into the environment. Out of the total heat supplied to an internal combustion engine in the form of fuel, approximately 30-40% is converted into useful mechanical work; the remaining heat is expelled to the environment through exhaust gas and engine cooling systems, resulting into entropy rise and serious environmental pollution. So it very important to utilize this waste heat into useful work. The recovery and utilization of waste heat not only conserves fuel but also reduces the amount of waste heat and greenhouse gases dumped into the environment. In this paper a detailed study has been presented about the various conventional and recent methods of refrigeration and air conditioning used for the recovery of waste heat from internal combustion engines.

Keywords: *waste heat recovery, vapour absorption refrigeration, adsorption*

## 1. INTRODUCTION

Waste heat can be defined as the heat which is generated in a process by way of combustion of fuel or chemical reaction, and then rejected into the environment even though it could still be reused for some useful and economic purpose. The essential quality of heat is not the amount but rather its "value". The strategy of how to recover this heat depends in part on the temperature of the waste heat gases and the economics involved. **Waste heat recovery** is the collection of **heat** created as an undesired by-product of the operation of a piece of equipment or machinery to fill a desired purpose elsewhere. Large quantity of hot flue gases is generated from Boilers, Kilns, Ovens and Furnaces. If some of this waste heat could be recovered, a considerable amount of primary fuel could be saved. The energy lost in waste gases cannot be fully recovered. However, much of the heat could be recovered and loss minimized by adopting various measures [3].

Depending upon the type of process, waste heat can be rejected at virtually any temperature from that of chilled cooling water to high temperature waste gases from an industrial furnace or kiln. Usually higher the

temperature, higher the quality and more cost effective is the heat recovery. In any study of waste heat recovery, it is absolutely necessary that there should be some use for the recovered heat. Typical examples of use would be preheating of combustion air, space heating, or pre-heating boiler feed water or process water. With high temperature heat recovery, a cascade system of waste heat recovery may be practiced to ensure that the maximum amount of heat is recovered at the highest potential

Out of the total heat supplied to an internal combustion engine in the form of fuel, approximately 30-40% is converted into useful mechanical work; the remaining heat is expelled to the environment through exhaust gas and engine cooling systems, resulting into entropy rise and serious environmental pollution. So it very important to utilize this waste heat into useful work. The recovery and utilization of waste heat not only conserves fuel but also reduces the amount of waste heat and greenhouse gases dumped into the environment.

Waste heat losses occur both from the equipment inefficiencies and thermodynamic limitations on

equipment and processes. For example, let us consider an internal combustion engine converting 30-40% of supplied energy into useful mechanical work. This implies 60-70% of the supplied energy is lost as waste heat. Exhaust gases leaving the engine can have temperatures as high as 400-600°C which means that these gases have high heat content. Figure 1.1 shows the total energy distribution of an internal combustion engine [19].

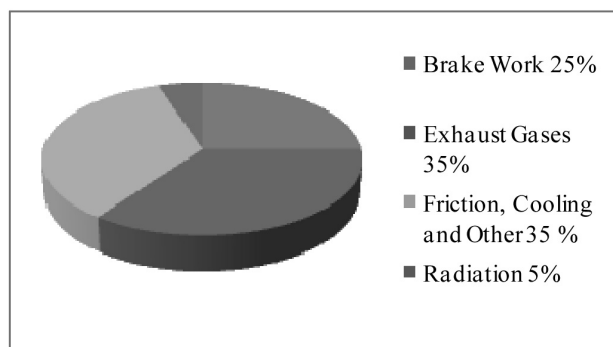


**Figure 1: Total fuel energy distribution in I.C Engine**

Heat recovery from automotive engines has been predominantly used for turbo-charging or for cabin heating and cooling with the application of absorption chillers. The basic objective of developing a vapor absorption refrigeration system for automobiles is to lower the temperature of a small space inside the vehicle by utilizing waste heat of the engine. The engine heat can be recovered either from the exhaust gas or from the radiator water. Hence, to utilize the exhaust gases and waste heat from an engine the vapor absorption refrigeration system can be put into practice which will increase the overall efficiency of the engine.

The main objectives of this study are:

- To study the feasibility of utilization of waste heat from the I.C. Engine for the purpose of refrigeration and air conditioning.
- To study about the various conventional and recent methods of refrigeration and air conditioning used for the recovery of waste heat from I.C. Engines.
- To study about a few experimental and computational works performed on the various refrigeration and air conditioning systems recovering waste heat from I.C. Engines.

## 2. LITERATURE REVIEW

A detailed literature review is available on the various techniques of recovering waste heat from internal combustion engines for the purpose of refrigeration and air conditioning. It is seen that in most of the studies, vapour

absorption system is used for the extraction of waste heat while in few studies vapour compression system and adsorption air conditioning system are also used for the heat recovery purpose. A detailed discussion of different experimental, theoretical and computational studies on the various technologies of waste heat recovery from internal combustion engines for refrigeration and air conditioning are presented section.

Manzela et al. [1] presented an experimental study of an ammonia-water refrigeration system using waste heat from an IC engine exhaust. The availability of exhaust gas energy and the impact of the engine performance due to the integration of vapour absorption refrigeration system, and power economy were evaluated. The engine was tested for 25 %, 50 %, 75% and wide open throttle valve. It was seen that the refrigerator had reached a steady state temperature between 4°C and 13°C about 3 hour after system start up, depending upon the throttle valve opening. The calculated exhaust gas energy availability suggests the cooling capacity can be highly improved for a dedicated system. The exhaust hydrocarbon emissions were higher when the refrigeration system was installed in the engine exhaust, but carbon monoxide emissions were reduced, while carbon dioxide concentration remained practically unaltered.

Khaled S AlQdah [8] presented an experimental study of an aqua-ammonia absorption system used for automobile air conditioning system using waste heat from a diesel engine. The estimated cooling load for the automobile found to be within acceptable ranges which are about 1.37 ton refrigeration. The obtained results showed that the COP values were directly proportional with increasing generator and evaporator temperatures but decrease with increasing condenser and absorber temperatures. The COP value was found in the range of 0.85 and 1.04.

Jotava et al. [17] recovered waste heat from the exhaust of an internal combustion engine and used it to run a Electrolux refrigeration system. The system was found to be applicable and ready to produce the required conditioning effect without any additional load to the engine. The proposed system decreases vehicle operating costs and environmental pollution caused by the heating system as well as causing a lower global warming.

Wang et al. [11] developed a mixed effect absorption chiller (AC) which recover heat both from the jacket water and exhaust gas. The high pressure generator is powered by exhaust gas while one low pressure generator is powered by jacket water waste heat. The thermodynamic characteristics and off design performance are simulated.

For 16 kW ICE, the cooling output had reached 34.4kW with COP of 0.96 and the exergy efficiency 0.186.

Wang et al. [10] applied a CCHP (Combined cooling heating power) system in a dual source powered mixed effect AC. The CCHP system integrates both fossil fuel energy and solar energy together. Refrigeration performance of this mixed effect AC under both waste heat mode and solar mode were tested and compared. In waste heat mode, the AC is simultaneously powered by exhaust gas waste heat and hot water from an ICE. In solar mode, the AC is powered by hot water from a solar thermal collector matrix. Test results show that the COP in waste heat mode is 0.91 while in solar mode it is 0.6.

Christopher et al. [6] investigated a single effect ammonia-water absorption system driven by heat rejected from a diesel engine. The waste heat is recovered using an exhaust gas heat exchanger and delivered to the desorber by a heat transfer fluid loop. The absorber and condenser are hydraulically coupled in parallel to an ambient heat exchanger for heat rejection. A thermodynamic model was developed for a baseline cooling capacity of 2kW and a detailed parametric study of the optimized system for both cooling and heating mode operation was conducted over a range of operating conditions. These parametric investigations showed that degradation of system performance can be limited, and improved COPs can be achieved by adjusting the coupling fluid temperature with the variation of ambient temperature. With the variation of return air temperature, the system was able to provide the 2kW design cooling capacity for the entire ambient temperature range.

Koehler et al. [1] designed and tested a prototype of absorption for truck refrigeration using heat from the exhaust gas. The refrigeration cycle was simulated by a computer model and validated by test data. The recoverable energy from the exhaust gas was analyzed the truck driving conditions at city traffic, mountain roads and flat roads. The prototype showed a coefficient of performance of about 27 %, but system simulation showed that it could be improved nearly by double.

Dong et al. [10] presented a novel idea of integrating a refrigeration and power system using Organic Rankine cycle (ORC) and solid sorption technology into internal combustion engines. A one dimensional engine model was coded using WAVE to evaluate the waste heat quantity of a medium duty diesel engine. The recoverable waste heat from the coolant and exhaust system has been analyzed under engine overall operational region. Based on these results, the working conditions of a cogeneration were

designed and the performance of the cogeneration was evaluated throughout the engine operating region. The system has the potential to improve the overall efficiency of the ICE from 40% to 47%.

S. Lakshmi [13] studied the use of energy from the exhaust gas of internal combustion engine to power a vapour absorption refrigeration system to air condition an ordinary passenger car. A preheater is employed to utilize the cooling water heat for preheating the  $\text{NH}_3$  solution flowing from absorber to generator. Thermal analysis of evaporator and condenser is done in ANSYS for aluminum alloy and copper.

Following are the observations on the basis of literature survey:

- A lot of research work has been carried out on the various technologies of waste heat recovery from internal combustion engines for the purpose of refrigeration and air conditioning.
- It is seen that in most of the research work, vapour absorption refrigeration system has been used for the purpose of waste heat recovery. This is because the engine exhaust gas is confirmed as a potential power source for absorption refrigeration systems.
- In a few studies it has been found that the domestic absorption refrigerator showed low COP (in the range 0.85- 1.04) and did not provide the cooling capacity needed for automotive application. However, a dedicated absorption refrigeration system may be able to take advantage of the exhaust gas power availability and provide the cooling capacity required for automotive air conditioning.
- It has been found from various studies that the COP of the absorption refrigeration system integrated with the exhaust system of ICE was directly proportional with the increasing generator and evaporator temperatures. However, the COP decreased with the increasing absorber and condenser temperatures.
- It is observed that with the installation of absorption refrigeration system the carbon monoxide emission was decreased, while the hydrocarbon emissions showed an increase.
- Introduction of refrigeration system in the engine exhaust system did not cause any significant pressure drop in the exhaust flow, as the engine output power was increased and specific fuel consumption was decreased.
- The various studies revealed that the installation of refrigeration system with the exhaust system of I.C. Engines decrease the vehicle operating cost, environmental pollution and global warming.



On the basis of detailed review of the literatures the following research gaps are identified:

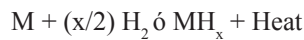
- A lot of research work on the waste heat recovery technologies from internal combustion engines for refrigeration and air conditioning has been performed with vapour absorption refrigeration systems. But the waste heat utilization on other refrigeration systems still requires further research work.
- A lot of experimental work has been performed on the waste heat recovery technologies for refrigeration and air conditioning but very little computer simulation work is performed in this field.
- The COP obtained from the refrigeration system used for the waste heat utilization gives a low value. So further research work is required for the improvement of COP.
- A lot of research work on waste heat recovery technologies for refrigeration and air conditioning has been performed on large scale stationary diesel engines but waste heat utilization on micro scale stationary diesel engines still require further research work. With the help of efficient heat exchangers there is a great chance to recover the exhaust waste of stationary diesel engines at every load and speed of the engine.

### 3. REFRIGERATION/AIR CONDITIONING TECHNOLOGIES FOR WHR IN I.C. ENGINES

The various refrigeration/air conditioning systems which can be utilized to recover waste heat from an internal combustion engines are listed below:

#### A. Metal hydride systems:

Metal hydride heat pumps utilize the fact that when hydrogen is adsorbed by the metal, heat is released because it is an exothermic reaction. The above process is reversible i.e. releasing the hydrogen is endothermic reaction. The desorption cooling step acts similar to the evaporator in vapour compression refrigeration system. In the equation given below, M represents the rare earth metal alloy and  $MH_x$  the metal hydride:



The basic operation of a hydride heat pump is shown in Figure 2 (for one particular configuration). The system consists of two metal hydride beds (a low temperature and high temperature metal), three heat exchanger sections (high, ambient and low temperatures). It cycles the beds through these heat exchangers over time to achieve cooling. Continuous cooling can be achieved by having four hydride beds [18].

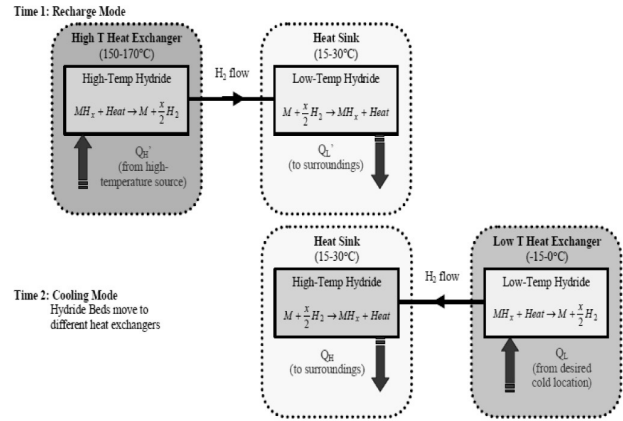


Figure 2: Basic operation of metal hydride heat pump

#### Advantages:

- This system has less number of moving parts compared to a conventional vapour compression refrigeration system, as the system does not require a compressor or evaporator.
- They have lower maintenance cost.
- Metal Hydride system does not require CFC for cooling.
- They occupy a smaller volume compared to the conventional system.

#### Disadvantage:

- Metal hydride system has a lower value of COP (0.4-2.5)

#### B. Zeolite Systems

- This system is similar to the metal hydride system, the only difference is that they use zeolite and water in the place of hydride and hydrogen. Zeolite is a natural mineral (e.g. porous aluminosilicate) and it has the property to absorb water vapour. Heat is released when the absorbed water vapour is incorporated in its internal crystal lattice.



- The zeolite system requires cycling between adsorption and desorption. The basic operation of a zeolite system is shown in figure 3. The sequence of adsorption/desorption process is reversible [4].

#### Advantages:

- The adsorption process of zeolites is very strong, thereby providing the family of materials with unique adsorption properties and permitting high efficiencies for adsorption heat pump cycles with air cooled condensers

- They provide heating and cooling at the same time.

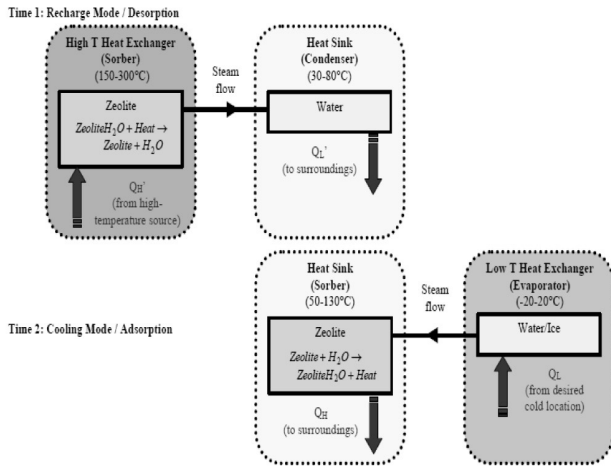


Figure 3: Basic operation of adsorption phase of zeolite system

*Disadvantages:*

- To provide continuous cooling, systems need to cycle between multiple sorption modules.
- To develop smaller components more research is needed to be performed.

**C. Thermoacoustics Systems**

These refrigerators use sound waves to pump heat. They are based on the fact that accompanying pressure and velocity changes with a sound wave are small temperature oscillations. With intense sound waves in suitable geometries, these thermoacoustic effects can be harnessed to produce powerful thermoacoustic engines and refrigerators. The sound level inside reaches upto 180dB, but outside the system is as quiet as a conventional AC system [18].

*Advantages:*

- Thermoacoustic generator appears attractive because of their elegance, reliability and low cost.
- They have no sliding parts and thus they do not require any lubrication.

*Disadvantages:*

- They have low efficiency and low power density.
- They are of large size.
- These devices are very sensitive.

**D. Thermoelectric Devices**

Thermoelectric Generator (TEG) is a device which converts thermal energy from different temperature gradients existing between hot and cold ends of a semiconductor into electric energy. In regards with the applicability of TEG in

modern engines, the ability of ICEs to convert fuel into useful power can be increased through the utilization of the mentioned device. Thermoelectric devices have highly desirable qualities for automotive refrigeration in their scalability, adaptability, reliability and lack of refrigerants [4].

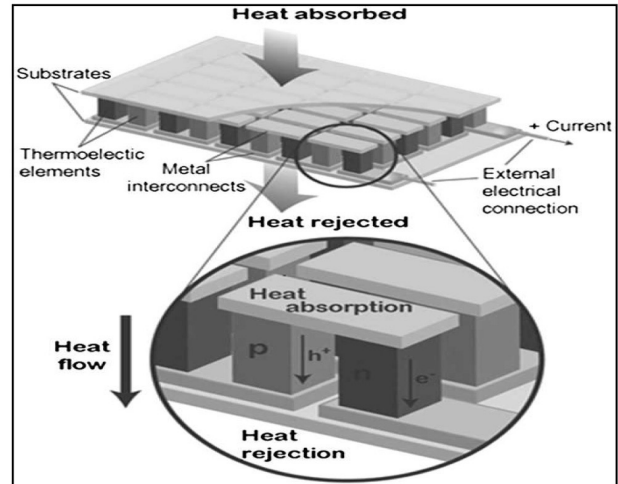


Figure 4: Schematic of a typical TEG

*Advantages:*

- They do not produce noise.
- Low maintenance cost.
- No moving parts.]

*Disadvantages:*

- Low thermal efficiency.
- Low cost.

**E. Absorption systems**

The vapour absorption refrigeration is one of the oldest methods of refrigeration which uses heat energy, instead of mechanical energy like in case of VCRS, in order to change the conditions of the refrigerant required for the operation of the refrigeration cycle. The vapour absorption refrigeration system consists of a condenser, an expansion valve and an evaporator similar to the vapour compression refrigeration system. But the compressor of the vapour compression refrigeration system is replaced by a generator, an absorber and a small pump. A vapour absorption refrigeration system utilizes two or more than two fluids which have high affinity towards each other, in which one of the fluid is a refrigerant and another one is the absorbent. The process of working of this refrigeration system is that a mixture of refrigerant and an absorbent is pumped from the absorber to the generator using a small pump. The generator supplies heat to the strong solution. Due

to this supplied heat, the refrigerant is separated from the strong solution and forms vapour. The remaining absorbent flows back to the absorber through a heat exchanger. The refrigerant in vapour state is then allowed to pass through a condenser where it loses heat and the temperature of the refrigerant drops to the ambient temperature. This cold refrigerant is passed through the evaporator from where the refrigerant absorbs heat and produces refrigerating effect. The refrigerant from the evaporator then moves to the absorber and mixes with the absorbent. Thus, the cycle continues [13].

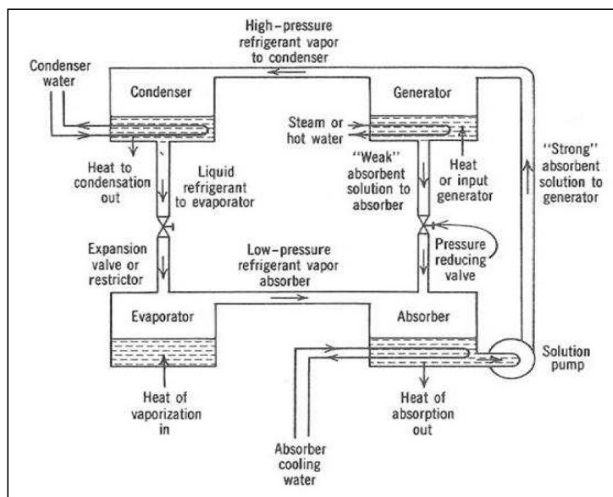


**Fig 5: Working of vapour Absorption Refrigeration Cycle**

#### Advantages:

- Compressor is not required.
- Lower maintenance cost
- Reduced atmospheric pollution.
- Low noise.

#### Disadvantages:

- High initial cost.
- Low working pressure. As a result COP is low.

#### IV. CONCLUSION

From the study it has been identified that there are large potentials of energy savings through the use of waste heat recovery technologies. The various technologies of refrigeration / air conditioning used for the purpose of waste heat recovery, offer great opportunities for reducing fuel use in vehicles. If these technologies are adopted then it would result in efficient engine performance and low emissions. Clearly there is a requirement for further analysis considering other aspects such as economic analysis that have not been considered in this paper.

#### V. REFERENCES

- [1] Manzela Andre A, Hanriaot Sergio Morais, Canbezaz-Gomez Luben, Sodre Jose Ricardo, *Using engine exhaust gas as energy source for an absorption refrigeration system*, Applied Energy 87, 2010, 1141-1148.
- [2] Talbi M, Agnew B, Energy recovery from diesel engine exhaust gases for performance enhancement and air conditioning, Applied Thermal Engineering 22, 2002, 693-702
- [3] Jiangzhou S, Wang R.Z, Lu Y.Z, Xu Y.X, Wu J.Y, *Experimental study on locomotive driver cabin adsorption air conditioning prototype machine*, Energy Conversion and Management 46, 2005, 1655-1665
- [4] Talom Huges L, Beyene Asfaw, *Heat recovery from automotive engine*, Applied Thermal Engineering 29, 2009, 439-444
- [5] Wu Chuang, Wang Shun-sen, Bai Kun-lun, Li Jun, Thermodynamic analysis and parametric optimization of CDTPC-ARC based on cascade use of waste heat of heavy duty internal combustion engines (ICEs), Applied Thermal Engineering 106, 2016, 661-673.
- [6] Keinath Christopher M, Delahanty Jared C, Garimella Srinivas, Garrabrant Michael A, *Diesel engine waste-heat driven ammonia-water absorption system for space conditioning applications*, International Refrigeration and Air Conditioning Conference, July 16-19, 2012.
- [7] Bhore Ketan, Bhosale Sharad, *Waste heat recovery of IC engine using VAR system*, International Engineering Research Journal, June 2016, 223-229, ISSN 2395-1621
- [8] AlQdah Khaled S, Performance and evaluation of aqua ammonia auto air conditioner system using exhaust waste energy, Energy Procedia 6, 2011, 467-476
- [9] AlQdah Khaled, Alsaqoor Sameh, Al-Jarrah Assem, *Design and fabrication of auto air conditioner generator utilizing exhaust waste energy from a diesel engine*, International journal of Thermal and Environmental engineering 3, 2011, 87-93
- [10] Lu Yiji, Wang Yaodong Dong Chenxuan, Wang Liwei, Roskilly Anthony Paul, *Design and assessment on a novel integrated system for power and refrigeration using waste heat from diesel engine*, Applied Thermal Engineering 91, 2015, 591-599
- [11] Wang Jialong, Wu Jingyi, Investigation of a mixed effect absorption chiller powered by jacket water and exhaust gas waste heat of internal combustion engine, International Journal of Refrigeration 50, 2015, 193-206

- [12] Wang Jialong, Wu Jingyi, Wang Hongbin, Experimental investigation of a dual source powered adsorption chiller based on gas engine waste heat and solar thermal energy, *Energy*, 2015, 1-10
- [13] Sowjanya S.Lakshmi, Thermal analysis of a car air conditioning system based on an absorption refrigeration cycle using energy from exhaust gas of an internal combustion engine, *Advanced Engineering and Applied Science: An International Journal* 3, 2013, 47-53
- [14] Mittal Atishey, Shukla Devesh, Chauhan Karan, *A refrigeration system for an automobile based on vapor absorption refrigeration cycle using waste heat from the engine*, *International Journal of Engineering Sciences & Research Technology*, 2015, 591-598
- [15] Maurya Satish, Awasthi Saurabh, Siddiqui Suhail, *A cooling system for an automobile based on vapour absorption refrigeration cycle using waste heat of an engine*, *International Journal of Engineering Research and Application*, 2014, 441-444
- [16] Manojprabhakar S, Ravindranath R.C, Vinothkumar R.V, Selvakumar A, Visagavel K, *Fabrication and testing of refrigeration using waste heat*, *International Journal of Research in Engineering and Technology*, 2014, 299-304
- [17] Jotava D.J, Parmar D.J, Shah Jay V, *Experimental investigation of heat recovery from engine exhausts gas and its application in Electrolux refrigeration system: A review*, *International Journal of Engineering Research & Technology* 3, 2014, 2560-2563
- [18] Johnson Valerie H., *Heat Generated Cooling Opportunities*, Society of Automotive Engineers, 2002-01-1969
- [19] Jadhoo JS, Thombare D.G, “Review on Exhaust Gas Heat recovery for IC. Engine”, *International journal of Engineering and innovative Technology*, 2, 2013, 93-100
- [20] Sonar D, Soni S.L., Sharma D, “*Micro-trigeneration for energy sustainability: Technologies, tools and trends*”, *Applied Thermal Engineering* 71 (2), 790-796.
- [21] Khatri KK, Sharma D, Soni S.L., Tanwar D “*Experimental investigation of CI engine operated micro-trigeneration system*” *Applied Thermal Engineering* 30 (11), 1505-1509

## DOCUMENT

# SWARAJ DAS (2015PTE5078)

## SCORE

**63** of 100

## ISSUES FOUND IN THIS TEXT

**525**

## PLAGIARISM

**6%****Contextual Spelling****82**

|                           |    |  |
|---------------------------|----|--|
| Misspelled Words          | 49 |  |
| Mixed Dialects of English | 19 |  |
| Confused Words            | 14 |  |

**Grammar****137**

|                                      |    |  |
|--------------------------------------|----|--|
| Determiner Use (a/an/the/this, etc.) | 90 |  |
| Wrong or Missing Prepositions        | 16 |  |
| Faulty Subject-Verb Agreement        | 11 |  |
| Incorrect Verb Forms                 | 5  |  |
| Incorrect Noun Number                | 4  |  |
| Faulty Tense Sequence                | 3  |  |
| Incorrect Phrasing                   | 3  |  |
| Misuse of Modifiers                  | 2  |  |
| Misuse of Quantifiers                | 2  |  |
| Conjunction Use                      | 1  |  |

**Punctuation****71**

|   |    |  |
|---|----|--|
| Comma Misuse within Clauses                 | 50 |  |
| Punctuation in Compound/Complex Sentences   | 19 |  |
| Misuse of Semicolons, Quotation Marks, etc. | 2  |  |

**Sentence Structure****13**

